Journal of General Virology

A Coxsackievirus B1-mediated nonlytic Extracellular Vesicle-to-cell mechanism of virus transmission and its possible control through modulation of EV release
--Manuscript Draft--

Manuscript Number:	JGV-D-23-00091R1
Full Title:	A Coxsackievirus B1-mediated nonlytic Extracellular Vesicle-to-cell mechanism of virus transmission and its possible control through modulation of EV release
Article Type:	Research Article
Section/Category:	Animal - Positive-strand RNA Viruses
Keywords:	Coxsackievirus B1; Extracellular Vesicles; Nonlytic transmission
Corresponding Author:	Jameel Inal, Ph.D. London Metropolitan University Faculty of Life Sciences: London Metropolitan University London, UNITED KINGDOM
First Author:	Samireh Jorfi, BSc PhD
Order of Authors:	Samireh Jorfi, BSc PhD
	Ephraim Abrokwa Ansa-Addo, BSc PhD
	Katia Mariniello, BSc PhD
	Purva Warde, BSc MSc
	Ahmad Asyraf bin Senian, BSc
	Dan Strattton, BSc PhD
	Bridget E. Bax
	Michelle Levene, BSc PhD
	Sigrun Lange, BSc MSc PhD
	Jameel Malhador Inal, Ph.D.
Manuscript Region of Origin:	UNITED KINGDOM
Abstract:	Like most non-enveloped viruses, CVB1 mainly uses cell lysis to spread. Details of a nonlytic virus transmission remain unclear. Extracellular Vesicles (EVs) transfer biomolecules between cells. We show that CVB1 entry into HeLa cells results in apoptosis and release of CVB1-induced 'medium-sized' EVs (CVB1i-mEVs). These mEVs (100-300 nm) harbour CVB1 as shown by immunoblotting with anti-CVB1-antibody; viral capsids were detected by transmission electron microscopy and PCR revealed CVB1 RNA. The percentage of EVs released from CVB1-infected HeLa cells harbouring virus was estimated from TEM at 34%. Inhibition of CVB1i-mEV production, with calpeptin or siRNA knockdown of CAPNS1 in HeLa cells limited spread of CVB1 suggesting these vesicles disseminate CVB1 virions to new host cells by a nonlytic EV-to-cell mechanism. This was confirmed by detecting CVB1 virions inside HeLa cells after co-culture with CVB1i-mEVs. Furthermore, CVB1-stimulated macropinocytosis enable the uptake of mEVs into HeLa cells following an endocytic pathway to late endosomes/lysosomes. EV release may also spread apoptosis to secondary sites of infection.
Author Comments:	I do NOT want open access, please. I had selected this originally because I thought my organisation had a Publish and Read agreement. I repeat I do NOT want open access but cannot find anyway on this portal to change this. I will need green access, subscription only. Thank you. My apologies.
Opposed Reviewers:	
Suggested Reviewers:	Amy Hartman Centre for Vaccine Evaluation

hartman2@cvr.pitt.edu

Ryan Langlois
University of Minnesota Medical School Duluth Campus: University of Minnesota Twin
Cities School of Medicine Duluth Campus
langlois@umn.edu

Silke Stertz
University of Zurich Institute of Virology: Universitat Zurich Virologisches Institut
stertz.silke@virology.uzh.ch

Additional Information:

Question	Response
Does this article report on work with humans or animals?	Not applicable (no human or animal experimentation is reported)
Does this article include details (names, inititals, hospital numbers), images, or videos relating to an individual person?	No

Click here to access/download
Response to Reviewer
Rebuttal_JGV_INAL.docx

A Coxsackievirus B1-mediated nonlytic Extracellular Vesicle-to-cell mechanism of virus transmission and its possible control through modulation of EV release

Samireh Jorfi[*,1], Ephraim Abrokwa Ansa-Addo[*,1,¶], Katia Mariniello[1,§], Purva Warde[2], Ahmad Asyraf bin Senian[2,†], Dan Stratton[3], Bridget E. Bax[4], Michelle Levene[4], Sigrun Lange[5,6] and Jameel Malhador Inal[1,2]

[1]Extracellular Vesicles in Disease Pathology, School of Human Sciences, London Metropolitan University, UK; [§]Current address: William Harvey Research Institute, Queen Mary, University of London. [2]Biosciences Research Group, School of Life and Medical Sciences, University of Hertfordshire, UK; [¶]Current address: Pelotonia Institute for Immuno-Oncology, The James, Ohio State University, U.S.A.; [†]Current address: Clinical Research Centre-Sarawak General Hospital, Malaysia; [3]School of Life, Health & Chemical Sciences, The Open University, UK; [4]Molecular and Clinical Sciences Research Institute, St. George's, University of London, UK; [5]University of Westminster, Tissue Architecture and Regeneration Research Group, School of Life Sciences, 116, New Cavendish St., London, UK; [6]University College London School of Pharmacy, Brunswick Sq., London.

*Equal contribution
Correspondence and requests for materials should be addressed to J.M.I. (email: j.inal@londonmet.ac.uk or j.inal@herts.ac.uk)

Abstract
Like most non-enveloped viruses, CVB1 mainly uses cell lysis to spread. Details of a nonlytic virus transmission remain unclear. Extracellular Vesicles (EVs) transfer biomolecules between cells. We show that CVB1 entry into HeLa cells results in apoptosis and release of CVB1-induced 'medium-sized' EVs (CVB1$_i$-mEVs). These mEVs (100-300 nm) harbour CVB1 as shown by immunoblotting with anti-CVB1-antibody; viral capsids were detected by transmission electron microscopy and RT-PCR revealed CVB1 RNA. The percentage of mEVs released from CVB1-infected HeLa cells harbouring virus was estimated from TEM at 34%. Inhibition of CVB1$_i$-mEV production, with calpeptin or siRNA knockdown of *CAPNS1* in HeLa cells limited spread of CVB1 suggesting these vesicles disseminate CVB1 virions to new host cells by a nonlytic EV-to-cell mechanism. This was confirmed by detecting CVB1 virions inside HeLa cells after co-culture with CVB1$_i$-mEVs; EV release may also prevent apoptosis of infected cells whilst spreading apoptosis to secondary sites of infection.

Introduction

Coxsackievirus B1 (CVB1) is a non-enveloped, single-stranded RNA enterovirus of the *Picornaviridae* family and is associated with a broad spectrum of human diseases including myocarditis, meningoencephalitis, pancreatitis and paralytic myelitis [1],[2]. Early during infection, in the gastrointestinal tract, Group B coxsackieviruses (CVB) encounter the polarized epithelium. To initiate an infection *in vivo*, CVB cross the intestinal mucosa, which is lined by polarised, epithelial cells. Infection of these cells requires interaction with the apically located decay-accelerating factor (DAF) [3-5]. This mediates attachment before the virus is transported to the basolaterally located coxsackie adenovirus receptor (CAR) where entry occurs by endocytosis [3-5]. Viral replication occurs in the mucosa followed by lysis of epithelial cells and subsequent viremia. However, CVB may also infect non-polarised cells such as HeLa, in which although DAF is expressed, viral interaction, mediated through DAF, is not necessary.

Many viruses manipulate their host cell death pathways to avoid premature death which would otherwise terminate viral replication. CVB4 for example utilises protein 2BC, which by association with caspase-3 inhibits its apoptotic role [6]. Other viruses such as CVB3 inhibit host cell apoptosis by preventing Bax and Bak-mediated permeabilization of mitochondrial membranes, and subsequent cytochrome c release, and pro-caspase-3 activation, through blocking with viral Bcl-2-like proteins (homologues of their mammalian counterparts) [7]. Once pro-caspase-3 is activated, however, apoptosis, is inevitable.

In the case of measles virus, infected monocytes induce apoptosis of uninfected T cells indirectly, through surface protein interactions [8]. Such bystander apoptosis where neighbouring (uninfected) cells undergo apoptosis is also an important part of the pathogenesis of infection with neurotropic cytomegalovirus, CMV [9]. Interestingly, some studies have suggested that CVB1-induced apoptosis of neighbouring cells does not exclusively occur by a lytic egress of enteroviruses and their spread [10, 11]. Indeed, this was suggested by earlier work showing intercellular spread of poliovirus in the CNS [12]. Similarly, work using CVB3 showed the virus to induce cellular protrusions which were believed to constitute a nonlytic (or prelytic) means of intercellular transmission [13].

Extracellular Vesicle (EV) subtypes include 'exosomes' of endosomal origin, plasma-membrane derived 'microvesicles' and apoptotic bodies. In the absence of knowledge of the specific biogenesis pathway, operational terms to subdivide EVs are based on size: small, medium and large EVs. Small EVs (sEVs) are 30-100 nm (expressing tetraspannins), medium EVs (mEVs) 100-200 nm and large EVs (>200 nm). To define sEVs as 'exosomes,' requires purification through a density gradient, recovering the sample at 1.13-1.19 g/mL and confirmation of various exosome markers [14] as there is an overlap with the size of medium EVs (mEVs). Exosomes are derived from endocytosis and intraluminal budding within endosomes and are released upon fusion of multivesicular endosomes with the plasma membrane [15]. Microvesicles are released by budding off the plasma membrane upon activation with extracellular stimuli such as sublytic complement, their release under the control of neutral sphinogomyelinases [16]. The release of vesicles is preceded by an increase of intracellular calcium ($[Ca^{2+}]_i$) [17]. This leads to activation of aminophospholipid translocases (flippase and floppase) [18] and calpain, as well as of peptidylarginine deiminases resulting respectively in: (i) loss of lipid asymmetry in the plasma membrane [18], (ii) depolymerization of the actin cytoskeleton and (iii) citrullination of actin [19]. mEV biogenesis also involves RhoA-mediated regulation of cytoskeletal rearrangements via the RhoA-cofilin pathway [20] and together with RacA this can switch between mEV release and extension of invadopodia [21-23]. Large EVs (300-1000 nm) include apoptotic bodies [14].

EVs in general participate in intercellular communication by carrying numerous proteins, miRNA, mRNA and lnRNA between cells [24, 25]. The release is also a way of shedding deleterious substances from cells such as misfolded proteins [26, 27] as well as chemotherapeutic drugs from tumour cells [28-30]. EVs may also play a role in autoimmune diseases by inhibiting the phagocytosis of apoptotic cells [31, 32]. Others have shown that

EVs can act as vehicles of immunosuppression [33], participating in cancer progression [34-36] and inflammatory responses [37] and they may furthermore spread apoptotic signals, as with monocyte-derived EVs able to induce apoptosis of vascular smooth muscle cells [38] via EV-borne caspase-1. Monocyte EVs may even play a role during monocyte terminal differentiation [39, 40]. Furthermore, EVs may participate in host-parasite interactions, leading to infectious disease [41] and plasma EV levels are raised by intracellular parasites such as *T. cruzi* [42] and in malaria infection [43].

The roles that mEV release play in the normal physiological processes of the cell are only slowly being unravelled [17, 44, 45]. We are also learning that this process is exploited by intracellular pathogens to enter host cells. Notably, we demonstrated recently that *T. cruzi* metacyclics induce host cell mEV release and that they are able to evade host complement-mediated lysis by fusing with such blood cell-derived mEVs [42, 46] and that mEVs from complement resistant parasites can transfer an invasive phenotype to wild type *T. cruzi* [47]. Conversely, the intestinal parasite *Giardia intestinalis* uses its own mEVs to help attach the trophozoite forms to Caco-2 intestinal epithelial cells and to increase activation and allostimulation of immature dendritic cells [48].

Picornaviruses disrupt the host cytoskeleton in the early phase of infection [49, 50] but also do so later on to facilitate virus release [51]. Disruption of the host cytoskeleton, as a result of depolymerization or maybe reorganization, also results in release of EVs [52-54]. As EVs are able to induce apoptosis of neighbouring healthy cells [38, 55, 56], this prompted us to investigate CVB1-mediated release of EVs from host cells and the role of these vesicles in the spread of CVB1-induced apoptosis. This study aimed initially to assess how CVB1 induces EV release from HeLa cells. We showed that CVB1 requires a calcium-mediated activation of calpain and disruption of the host cytoskeleton, during CVB1-mediated EV release, and for infection. Upon entry, CVB1 causes further release of CVB1-induced HeLa EVs (CVB1$_i$-mEVs) from infected cells. Following on from our original findings into the role of host EVs in CVB1 infection [57-59], we investigated whether virally infected cells release EVs able to induce apoptosis. We hypothesized that while EV release from infected cells may spread apoptosis to uninfected host cells and so limit virus spread, viruses may also use this pathway for active dissemination. By better understanding the mEV-mediated mEV-to-cell means of viral transmission, and its relative contribution to overall viral transmission, it may be possible to focus on novel strategies to inhibit viral spread between cells.

Materials and Methods

Cell culture

HeLa cells (ECACC, 93021013) were maintained at 37 °C (5% CO_2 humidified conditions) in DMEM supplemented with 10% EV-free FBS, 2 mM L-glutamine, 1% non-essential amino acids, 100 U/ml penicillin, and 100 mg/ml streptomycin (complete growth medium, CGM). The FBS in CGM was substituted for Extracellular Vesicle- (EV-) free FBS (centrifuged at 100,000 ×*g* for 18 h) [17, 28], 18 h before the EV collection period. The HeLa cells used were routinely screened for *Mycoplasma* using the MycoProbe Mycoplasma Detection Kit (R&D Systems) and found to be free of contamination. Exponentially growing cells were counted and viability determined using the Guava ViaCount Reagent by flow cytometry (ViaCount assay; EMD Millipore) as described before [19, 60]. After three days in culture, cells were routinely split 1:4 at about 80% confluence, and only cultures with at least 95% viability were used in experiments.

CVB1 propagation, purification and EV depletion

Coxsackievirus B1 (CVB1) (Batch No: NCPV 231) was obtained from the Health Protection Agency (HPA, UK) and expanded by infecting HeLa cells (not exceeding a passage number of 30) to prepare viral stocks. Confluent cultures of HeLa cells were infected at an MOI (multiplicity-of-infection) of 10 and after overnight incubation at 37 °C harvested by adding 0.1% v/v Tween 80 in PBS and by three freeze/thaw cycles. Cell debris was then removed by centrifugation of the supernatant at 1,000 ×*g* for 15 min, and further centrifugation of the supernatant at 11,000 ×*g* for 30 min was followed by filtration through a 0.22 µm pore size filter. The virus was purified by pelleting at 65,000 ×*g* for 18 h through a 30% sucrose cushion (prepared in SM buffer; 50 mM Tris, pH 7.4, 100 mM NaCl, 10 mM $MgSO_4$) and stored at -80 °C. When EV-depleted CVB1 was required, such as where CVB1 provided the stimulus for macropinocytosis, naked CVB1 virions were depleted of EVs by incubating with 0.1% triton, prior to density gradient centrifugation using a 10-25% sucrose gradient (40,000 ×*g* for 90 min; SW-41 rotor) followed by fractionation. Peak VP1-containing fractions, ascertained by western blotting (Fig. S1) were pooled and either centrifuged at 100,000 ×*g* for 2 h or precipitated using trichloroacetic acid, pellets being resuspended in PBS buffer. Sucrose gradients were similarly used to isolate mEVs free of virus.

CVB1 plaque assay on HeLa cells

Titres of purified CVB1 were determined using an agar overlay plaque assay on HeLa cells. HeLa cells ($5×10^4$cells/well) were seeded into 12-well plates and incubated at 37 °C, 5% humidified CO_2 for 24 h. Cells were washed twice with RPMI and resuspended in CGM. The CVB1 stock was serially diluted in 10-fold steps and added to the 90-95 % confluent cell monolayer; cells were also sham-infected with PBS as a negative control. After incubation at 37 °C, 5% CO_2 for 4 h, cells were overlaid with 0.6% agarose and then incubated for 5 days (37 °C, 5% CO_2). The overlay medium was removed carefully, and the cells fixed by resuspending in 4% paraformaldehyde (15 min, RT). After washing with PBS, cells were stained using 0.2 % crystal violet (1h at RT), washed twice with tap water and plaques then counted. The virus of known titre (calculated in PFU/ml) was stored at -80 °C. For infection, cells were inoculated with CVB1 at an MOI of 5 and kept at 37 °C until fixation for flow cytometry or for performing immunofluorescence assays.

Antibodies and chemicals

CVB1 was detected using mouse anti-CVB1 monoclonal antibody (mAb) MAB944 (clone 334-4A-8F-3F), (Chemicon Int. Inc., CA, USA). Flow cytometry analysis of cell associated viral proteins was carried out with anti-CVB1 mAb (MAB944) followed by Alexafluor 488-conjugated anti-mouse IgG (Life Technologies Ltd, Paisley, UK) referred together as 'anti-CVB1 Alexafluor 488' antibody. Antibodies to CD9 and CD81 were from R&D Systems and for TSG101 and syntenin-1 from Invitrogen (Thermo Fisher, UK). The β-actin monoclonal antibody was obtained from Sigma-Aldrich (Haverhill, UK) as was the anti-CAPNS1 mAb; β-tubulin was from Invitrogen (Thermo Fisher Scientific Cat# # 32-2600, RRID: AB_2533072). The rabbit anti-active caspase-3 monoclonal antibody (A5-32015) and rabbit monoclonal against procaspase-3 (MA5-32027) were both from Thermo Fisher. Mouse anti-CAR (clone RmcB, Upstate®) and the isotype control, mouse IgG1, were purchased from Sigma-

4

Aldrich. Neutralizing mouse anti-CVB1 (as opposed to that used for detection, above) was obtained from Merck & Co. (mouse anti-CVB1 mAB, MAB944) and used at 62.5 μg/ml in *in vitro* infection experiments. Calpeptin was from Merck Biosciences (Germany).

Isolation of mEVs from HeLa cells upon stimulation with CVB1
To ascertain whether CVB1 could stimulate mEV release, semiconfluent HeLa cells seeded at 5×10^4 cells/well in 12-well plates were serum-starved overnight (0.1% v/v EV-free FBS), washed (3X in serum-free medium (SFM)) and were then infected with CVB1 (MOI 5; 5 PFU/cell) at 37 °C in SFM to eliminate contamination with bovine EVs for 2 or 12 h. Where necessary, cells were pretreated with calpeptin or BAPTA-AM or the pan-caspase inhibitor, Z-VAD-fluoromethyl ketone (zVAD) all at 20 μM for 45 min. Cells were then washed with DMEM three times to remove any unbound virus, resuspended in CGM (prepared using EV-free FBS (centrifuged at 100,000 ×*g* for 18 h) as described under 'cell culture') and incubated at 37 ˚C, 5% CO_2 for 2 or 12 h. Conditioned medium from infected cells was collected after 2 h and 12 h, but with hourly removal and re-supplementation with EV-free CGM (between 2 and 12 h). EVs were isolated and quantified by first centrifuging at 160 ×*g* for 5 min to pellet cells. The supernatant was further centrifuged twice at 4,000 ×*g* for 30 min to remove cell debris. The resultant supernatant was then centrifuged at 11,000 ×*g* for 60 min to pellet mEVs. Pelleted mEVs were resuspended in sterile EV-free PBS [19] and washed twice by further centrifugation at 11,000 ×*g* for 60 min. Finally, isolated mEVs were resuspended in sterile EV-free PBS and quantified using nanosight tracking analysis as described before [61], and below. These mEVs (CVB1i-mEVs) released from CVB1-induced HeLa cells were also used in further infection experiments. For isolation of sEVs ('exosomes'), the resultant supernatant was centrifuged at 100,000 ×*g* for 1h. Exposure of phosphatidylserine (PtdSer) was monitored by determining binding of AnV-FITC to EVs. This was carried out as described before [19].

Particle size distribution using Nanoparticle Tracking Analysis (NTA) of mEVs and sEVs released from HeLa cells
The m/sEV samples were diluted 1/1500 using EV-free RPMI, and the size distribution and concentration then determined by nanoparticle tracking analysis (NTA) using a Nanosight NS300 (Nanosight, U.K.) as described before [19, 43, 60, 62]. The particles were quantified for size and number and represented on a frequency size distribution graph.

Measuring intracellular Ca^{2+} concentrations and membrane permeabilization
This was carried out as described previously using the cell permeant, high affinity calcium indicator Fura 2-AM (Sigma-Aldrich) [45]. Essentially HeLa cells were loaded with Fura 2-AM in HEPES buffer (Ca^{2+}-free) and infected at MOI 10 and fluorescence readings taken. Any real-time alteration in plasma membrane permeability due to the cytotoxic action of BAPTA-AM (in experiments to measure intracellular calcium) was assessed using the intercalating agent propidium iodide (120 μM) (Sigma Aldrich). Propidium iodide in complex with DNA/RNA was detected at an emission of 610 nm under excitation of 539 nm. These experiments were carried out in triplicate.

Knockdown of CAPNS1 *by small interfering RNA (siRNA) transfection*
GeneSolution siRNA sequences targeted to four different sites in *CAPNS1* mRNA (GenBank Accession No. X04106.1) and negative control siRNA (Qiagen, Crawley, UK) were reconstituted in sterile RNase-free water at a final concentration of 10 μM. For CVB1 infection experiments, HeLa cells (5×10^4 cells/well in triplicate) were transfected with 50 nM siRNA, using HiPerfect transfection reagent (HPP, Qiagen) for 48 h, prior to performing experiments. The sequence for the human *CAPNS1* siRNAs were: siRNA**#1**, 5' -CAC CTG AAT GAG CAT CTC TAT - 3'; siRNA**#3**, 5' -AAG GTG GCA GGC CAT ATA CAA -3'; siRNA**#5**, 5' -CAG CGC CAC AGA ACT CAT GAA -3'; siRNA**#6**, 5' -TCC GAC GCT ACT CAG ATG AAA -3'. Negative control siRNA was: 5' -AAT TCT CCG AAC GTG TCA CGT -3'. Consistent reduction of CAPNS1 expression was observed with siRNA**#6**, and so siRNA**#6** was used to assess the effects of decreasing CAPNS1 levels on the sensitivity of HeLa cells to CVB1 induction of CVB1i-mEVs and apoptosis.

In vitro *apoptosis assay*

For all infection experiments with CVB1, HeLa cells were first plated at 37 °C for 48 h in CGM (as prepared above). For studying apoptosis induced by CVB1 or CVB1-induced HeLa EVs (CVB1$_i$-mEVs), semiconfluent HeLa cells were washed prior to addition of CVB1 or CVB1$_i$-mEVs. To investigate the role of calpain, calpeptin (20 µM) was added for 45 min prior to addition of CVB1. HeLa cells were also pre-treated with zVAD (20 µM for 45 min). HeLa cells were inoculated with CVB1 (MOI 5, throughout) or CVB1$_i$-mEVs at 1:1, 5:1 or 10:1 (EVs-to-cell ratios) (1h/37 °C to allow virus or EV adsorption) and incubated at 37 °C for 12 h with hourly removal of growth medium. In some experiments, HeLa cells ($5×10^4$ cells/well) were washed in serum-free DMEM and then seeded in 12-well plates and resuspended in complete medium; the cells at semi-confluence were co-cultured with 'DEX-mEVs,' EVs released from cells treated with dexamethasone (DEX) (Sigma-Aldrich) at 1 mM for 3 h at 37 °C to induce apoptosis. After 24 h apoptosis was determined by staining cells with Guava Nexin® reagent (which used annexin V-PE to detect externalised phosphatidylserine and 7-Aminoactinomycin D (7-AAD), a cell-impermeant dye to indicate late apoptosis) as described before [31]. After incubation for 30 min with mixing, the cells were analysed on a Guava EasyCyte 8HT flow cytometer. Induction of apoptosis was also confirmed by immunoblotting lysates of HeLa cells prepared as described below for the presence of activated caspase-3 and pro-caspase-3. Following CVB1 infection, HeLa cells were also examined for morphological changes by phase contrast microscopy.

Immunoblotting analysis

For detection of intravesicular virus. HeLa cells were pre-treated with 0.075% trypsin for 30 min at 37 °C to remove any surface bound virus, followed by three washes with cold EV-free PBS. Control or CAPNS1 knocked down HeLa cells, and purified EVs were lysed with lysis buffer (100 mM HEPES/KOH, 2 mM CaCl$_2$, 0.5% Triton X-100) containing protease inhibitor cocktail (Sigma-Aldrich, Haverhill, UK). The protein concentration of lysates was measured using the BCA assay kit (Pierce Biosciences, UK) and 20 µg (an equal loading of different sEV or mEV samples as well as cell lysates) was resolved by SDS-PAGE on a 12% polyacrylamide gel. Immunoblotting was carried out as described before [63] by transferring proteins to nitrocellulose membrane (Amersham Biosciences, GE Healthcare, Buckinghamshire, UK) at 100 mA, constant current for 1 h using the semidry transfer system (BioRad, UK). Blots were blocked overnight at 4 °C in 6% non-fat milk dissolved in PBS, and then incubated with the murine monoclonal antibodies anti-CVB1 (EMD Millipore, UK), anti-β-actin (Sigma-Aldrich, Haverhill, UK), or anti-calpain small subunit 1 (CAPNS1) (Sigma-Aldrich, Haverhill, UK), diluted 1/500 in PBST (PBS with 0.1% (v/v) Tween 20). Blots were washed six times in PBST for 10 min each time, and membranes were then probed with the secondary antibodies, anti-mouse-HRP (or anti-rabbit-HRP) (1/1000). After 1 h at room temperature (RT) with shaking, blots were washed six times in PBST for 10 min each. Protein bands were visualised using the LumiGOLD ECL western Blotting Detection kit (SignaGen Laboratories, Rockville, MD 20850), and the chemiluminescence signal detected using the ChemiDoc-It Imaging System (UVP, LLC, Cambridge, UK). When western blotting was carried out to distinguish mEVs and sEVs, the primary antibodies used were against: CD9 and CD81 (R&D Systems, UK), TSG101 and syntenin-1 (Invitrogen [Thermo Fisher] UK) and β-actin (Sigma Aldrich, Haverhill, UK). To detect apoptosis of HeLa cells in infection experiments, a rabbit monoclonal anti-active caspase-3 antibody and anti-procaspase-3 antibody (both at 1:1,000 from Thermo Fisher) were used. For westerns probed with more than one antibody, after rinsing the nitrocellulose in water, it was incubated in stripping buffer (62 nM Tris.HCl (pH 6.8); 2% SDS and 0.8%v/v β-mercaptoethanol) with gentle mixing (50 °C/30 min, washed in PBST (×6, 10 min each), blocked and reprobed. CVB1 (VP1) protein (34 kDa) and activated (or cleaved) caspase-3 protein levels (17 kDa) as well as those of pro-caspase-3 (32 kDa) were analysed and quantified densitometrically using ImageJ software [64]. The relative levels of CVB1 (VP1) and activated caspase-3 were normalised to β-actin, all western blotting experiments being carried out in duplicate. When probing mEV proteins in a western blot, instead of using β-actin as a loading control, total proteins were stained with MemCode (Thermo Fisher) according to the manufacturer's instructions.

Immunofluorescence detection of CVB1

For flow cytometry analysis, HeLa cells (5×10^4 cells/well) were plated into 12-well dishes 48 h prior to infection. Cells, when 80-90% confluent, were washed and then infected at an MOI of 5, incubating at 37 °C for 1h, for virus adsorption. After removal of any residual virus by washing, cells were incubated at 37 °C for 12 h, with hourly replacement of cell culture supernatant; cells were then washed, treated gently with trypsin, fixed and then permeabilised using the Fix and Perm Cell Permeabilization kit (ADG, Germany) according to the manufacturer's instructions. During permeabilization, cells were incubated with anti-CVB1 antibody (5 µg/ml) at RT for 30 min with shaking, in the dark. Cells were washed three times (400 ×*g*, 5 min) with cold PBS and stained with mouse anti-IgG-FITC (1/200) diluted in PBS with 3% BSA, for 30 min at RT, with shaking. After washing three times with PBS, cells were analyzed by flow cytometry using a Guava EasyCyte 8HT with GuavaSoft™ 3.3 software, to determine intracellular viruses.

For fluorescence microscopy, HeLa cells were seeded overnight in 12-well plates containing 18 mm coverslips. Semiconfluent cells were inoculated with CVB1 at an MOI of 5 and incubated at 37 °C for 1 h, washed to remove residual virus and then incubated at 37 °C for 12 h, with hourly replacement of cell culture supernatant; cells were fixed and permeabilised as described above and labelled at RT for 30 min with anti-CVB1 antibody (10 µg/ml) diluted in 3% BSA in PBS. After washing three times with PBS, cells were resuspended in 3% BSA in PBS containing Alexafluor 488 anti-IgG antibody (1/200) and incubated at RT for 1 h with shaking. Plates were washed three times and coverslips inverted on to microscope slides using DAPI-Vectashield (Vector Laboratories, Burlingame, CA). Images were captured using a fluorescent microscope (IX81 motorized inverted fluorescent microscope, Olympus). Where necessary, bright field and fluorescent images were overlayed using Fiji software (ImageJ, NIH, version ImageJ 1.5.3) [64].

Transmission electron microscopy (TEM) (negative staining and cross-sectional TEM)

EVs isolated by differential centrifugation were stained with 2% phosphotungstic acid (pH 6.8) or aqueous uranyl acetate, together with aqueous bacitracin. The sEV or mEV samples were then transferred to a 400-mesh copper grid (Agar Scientific) with a Pioloform support film (Agar Scientific) where they were treated with aqueous Alcian blue 8GX (1%) for 10 min. The sections were examined using a Hitachi H-7100 Transmission Electron Microscope (Olympus, Tokyo, Japan) and digital images were then acquired with an AMT digital camera.

CVB1-stimulated sEV uptake in HeLa cells was visualised by cross-sectional TEM. Here, cells were fixed by incubating in 3% glutaraldehyde in 0.1 M sodium cacodylate buffer (pH 7.2) for 1 h at RT and then incubated for 1 h at 0 °C in osmium tetroxide (1:1 mixture of 2% osmium tetroxide and 0.2 M sodium cacodylate). After block staining in 1% uranyl acetate, samples in 1% hot agarose were dehydrated in an ascending ethanol series (70% to absolute ethanol) and then washed in propylene oxide. After infiltration with a 1:1 mixture of propylene oxide:agar resin, left rocking for 16 h at RT, samples were embedded in capsules and polymerised (24 h at 60 °C). After cutting sections on a Leica ultramicrotome and staining in Reynolds lead citrate, they were examined by TEM using a JEOL JEM-1200 EX II electron microscope (JEOL, Peabody, MA).

Viral RNA extraction, Reverse Transcription and RT-PCR

To obtain RNA complex-free EVs or cells, they were treated with proteinase I (50 ng/µl; 15 min/37 °C). The reaction was then stopped with PMSF (5 mM; 10 min/RT, then 5 min/90 °C) before adding RNase I (500 ng/µL; 20 min/37 °C). RNA was then extracted using TRI Reagent (Sigma-Aldrich, UK) according to the manufacturer's instructions. Essentially, EVs were lysed using 1 ml of TRI Reagent. Samples were left standing for 5 min at RT. Subsequently, 0.2 ml of chloroform, for each ml of TRI Reagent used, was added to each sample. The samples were shaken vigorously for 15 s, and allowed to stand for 8 min at RT. The resulting mixture was separated at 11,000 ×*g* for 15 min at 4 °C to induce separation of the mixture into three phases: a red organic phase (containing protein), an interphase (containing DNA), and a colourless upper aqueous phase (containing RNA). The aqueous phase was transferred to a fresh tube containing 0.5 ml of isopropanol per ml of TRI Reagent used.

The samples were mixed and allowed to stand for 6 min at RT and then centrifuged at 11,000 ×*g* for 10 min at 4 °C. The precipitated RNA was washed in 75% ethanol at 11,000 ×*g* for 5 min at 4 °C and dissolved in 50 µl of diethylpyrocarbonate-treated water. The purity and concentration of RNA of each sample was assessed at 260 and 280 nm using a nanodrop. RNA was considered pure when the ratio of absorbance readings at 260 and 280 nm was in the range of 1.7-2.1. Additionally, RNA purity was detected by gel electrophoresis.

2 µg of RNA was converted to cDNA, using MultiScribeTM reverse transcriptase, in 20 µl reaction volumes, according to the instructions of the high capacity cDNA reverse transcription kit (Invitrogen, UK). PCR reactions were set up in 25 µl reaction volumes using Crimson Taq Reaction buffer (5 µl) (Biolabs, U.K.), 10 mM dNTPs (0.5 µl), 10 µM Forward/Reverse primers (0.5 µl each), Crimson Taq DNA polymerase, (0.125 µl), up to 25 µl with nuclease-free water. The primers used were: SET2, Forward **EVF3** 5'-CCCTGAATGCGGCTAATCC-3', Reverse **KS2** 5'-TTCAAGCCAGTCTCATGTGC-3' and SET3, Forward **EVF3** 5'-CCCTGAATGCGGCTAATCC-3' and Reverse **EV2** 5'-ATTGTCACCATAAGCAGCCA-3'. The PCR conditions for SET2 were: 95 °C, 30 s, [denaturation 95 °C, 30 s; annealing 54 °C, 45 s; extension 68 °C, 60 s] x40; 68 °C, 5 min; 4 °C, ∞. A second PCR (from SET2) was run as follows: PCR products were diluted 1:100 and 1 µl was added to the master mix (prepared as previously explained). The PCR conditions for SET3 were: 95 °C, 30 s followed by [denaturation 95 °C, 30 s; annealing 50 °C, 45 s; extension 72 °C, 60 s] x40; 68 °C, 5 min; 4 °C, ∞. Each RT-PCR analysis included two positive controls consisting of cDNA from RNA extracted from CVB1 and infected HeLa cells. To verify the absence of contamination, RT-PCR analysis also included a negative control of amplification consisting of 5 µl of sterile water, which was added in place of test sample.

Detection of RT-PCR amplicon
An aliquot of amplified RT-PCR product (10 µl) was subjected to electrophoresis at 80 V in a 2% agarose gel containing 0.05 µl/ml of 10 mg/ml ethidium bromide (Sigma-Aldrich, UK) and a 100 bp DNA Ladder (Fisher BioReagents, UK) was used as a molecular-weight marker. DNA bands were observed under ultraviolet illumination (UVP, LLC).

PKH67 labelling of mEVs
Washed mEVs (equivalent to 100 µg protein) and as a control a sample lacking mEVs, were labelled with PKH67 (Sigma-Aldrich) (diluted 1:1, v/v with Diluent C) for 45 min at 37°C and the reaction quenched with EV-free FBS. The sample was then washed once (15,000 ×*g* / 60 min) a second time through an OptiPrep™ density gradient, and a final wash in EV-free PBS, as before, to remove unincorporated dye, finally being suspended in 100 µl PBS.

Assay for macropinocytosis of PKH67-labelled mEVs in HeLa cells
The macropinocytosis assay for monitoring the uptake of fluid or mEVs, was based on protocols to quantitatively assess macropinocytosis in cell lines [65, 66]. Firstly, HeLa cells at 65-70% sub-confluency, growing in 24-well dishes on poly-L-lysine-coated circular coverslips were prepared. To stimulate macropinocytosis, 2,000 cells/well were washed in serum-free medium and then exposed to EV-free CVB1 (prepared as described under 'CVB1 propagation, purification and EV depletion') at an MOI of 50, for 60 min at 4 °C. Sham treated cells were given growth medium alone. After washing off unbound virus, the cells were incubated with 1 mg/ml Dextran-FITC to visualise macropinosomes (MPs); this was taken as t = 0. After specified periods at 37 °C, cells were fixed with 4% paraformaldehyde (PFA) in 0.25 M HEPES (5 min/20 °C) and images taken using an LSM5 Pascal, Carl Zeiss laser scanning confocal microscope. In some experiments cells (2,000 cells/well), that had been serum-starved for 30 min to minimise any basal macropinocytosis, were exposed to: (i) PKH67-mEVs (5×10^8) and 100 µg/ml Dextran-Texas Red (70 kDa) for up to 15 min for experiments to co-localize PKH67-mEVs (10 µg protein) to macropinosomes or MPs (Dextran-Texas Red-labelled intracellular vesicles near the surface) and (ii) for up to 60 min to localise endocytosed PKH67-mEVs or MPs (Dextran-FITC) along the endocytic pathway with 50 nM LysoTracker™ Red DND-99, henceforth termed Lysotracker (Thermo Fisher). Any unattached mEVs were

removed by washing the cells in cold PBS which were then fixed for 5 min with 4% PFA in 0.25 M HEPES at the time points indicated in the results.

In some experiments, uptake of PKH67-mEVs and of Dextran-FITC of HeLa cells pre-stimulated and then washed to remove unbound CVB1, was monitored by flow cytometry. The mean fluorescence index (MFI) was obtained using a Guava EasyCyte 8HT flow cytometer for at least 10,000 cells and the percentage uptake of mEVs in cells was normalised to values obtained for control, untreated cells. Macropinocytosis assays were also carried out at 4 °C to account for mEVs not taken up but remaining on the cell surface and to therefore more accurately calculate uptake. Where looking to inhibit macropinocytosis, cells were exposed to the following inhibitors (all from Sigma-Aldrich) for 30 min at 37 °C: trypsin (0.2% w/v); unlabelled An-V (150 µg/ml); MβCD (5 mM); amiloride (1 mM); 5-(N-ethyl-N-isopropyl)amiloride (EIPA) (1 mM); dynasore (80 µM); bisindolylmaleimide (10 µM); cytochalisin D (2 µM) or nocodazole (10 µg/ml).

Image processing and analysis
For Pearson's colocalization coefficient (r_p) [67], confocal fluorescent images were analyzed with JACoP [68], a plugin in ImageJ [64]. Each data point represents the analysis of 25 cells.

Statistical analysis
GraphPad Prism software, version 7.0 (GraphPad Software, San Diego, CA) was used in performing all statistical analysis. Data are presented as standard deviation (SD) based on experiments carried out 2 or 3 times (N=2 or 3), with triplicate readings (n=3). Unless otherwise stated, *P* values were 2-sided. Significance values: ns (non-significant), P > 0.05. The following were considered statistically significant differences: * P ≤ 0.05; ** P ≤ 0.01; *** P ≤ 0.001 and **** P ≤ 0.0001. Where multiple groups were compared, one-way ANOVA was used followed by Bonferroni's post-hoc.

Results

CVB1 induces a calcium-mediated release of mEVs from HeLa

It is now well established that physical and chemical insults on cells, can result in a calcium-mediated release of EVs. Examples of stimuli include deposition of sublytic levels of membrane attack complex pores (C5b-9), ATP-mediated activation of P2X7 receptors, calcium ionophore treatment of cells, infection with intracellular protozoan parasites such as *Trypanosoma cruzi* or *Plasmodium falciparum*, intracellular bacteria (*Salmonella enterica* serovar Typhimurium), by exposure to Extremely Low Frequency Magnetic Fields and by conditions of hypoxia and acidosis [19, 24, 42, 43, 69-71]. In the present study, we wanted initially to ascertain whether cells undergoing infection with CVB1 would release EVs.

We found that CVB1 induced the release of mEVs from HeLa cells (Fig. 1A) 2 h post infection (p.i.) and at non-significantly higher levels 12 h p.i., and that this release up to 2 h could be reduced to basal levels by prior incubation with calpeptin (CP). BAPTA-AM, the intracellular calcium chelator, also abrogated mEV release without any cytopathic effect on the HeLa cells (neither causing apoptosis after 2 h, Fig. 1B), nor inducing cell membrane permeabilization as detected by a lack of change of intracellular fluorescence with propidium iodide (dotted line in Fig. 1C). We did not assess whether CP-mediated inhibition of mEV release was specific to virus-induced release (as opposed for example to low pH/hypoxia-mediated mEV release). To ensure that the observed mEV release was not due to cellular proteins released during preparation of virus, a lysate of HeLa cells prepared by freeze-thawing, but lacking virus, was unable to stimulate mEV release from HeLa cells (Fig. 1A).

We also showed that the CVB1-induced release of mEVs (CVB1$_i$-mEVs) accompanied an increase of intracellular calcium in HeLa cells (Fig. 1C). Measured using Fura 2-AM, $[Ca^{2+}]_i$ reached 350 nM at 2 min, and could be reduced by chelation of intracellular calcium with BAPTA-AM (Fig. 1C). We were able to confirm, according to nanosight tracking analysis (NTA), representative plot shown in Fig. S2A, that mEVs (11,000 ×g centrifugation) lay in the size range 50 - 350 nm with modal peaks at 180 and 250 nm (Fig. S2A). Exosomes or small EVs (sEVs), (100,000 ×g, having removed the 11,000 ×g mEV pellet), and purified by sucrose density gradient centrifugation as described before [42], were collected for comparison (Fig. S2B) and lay in the narrower 30 - 150 nm range, with a modal peak of 90 nm. Exosomal markers (TSG101, syntenin-1, CD81 and CD9) were crucially absent in the mEVs (collected at 11,000 ×g), Fig. S2C. β-actin has been found by others to be in mEVs [72, 73] but not in exosomes [73-76] as might be expected given the importance of cytoskeletal remodelling in mEV biogenesis [29, 52]. Its absence in the exosomal preparation also points to the sample being relatively devoid of cellular debris. AnV binding was also higher in mEVs indicating a high exposition of phosphatidylserine (Fig. S2D) [73] and electron microscopy (Fig. S2D) confirmed the sizes noted above by NTA.

Downregulation of calpain expression inhibits mEV production, CVB1 ~~entry~~ infection and virus-elicited apoptosis in HeLa cells

Activation of calpain plays a role in viral egress and entry. Previous reports have described an increase in calpain activity prior to reovirus-induced apoptosis and shown that inhibiting calpain protects against virus-induced myocardial cell death [77], whilst preventing release of virus progeny post-infection [78]. As well as playing a role in viral egress, activation of calpain plays a role in virus entry, the first step of infection in the viral life cycle. Other work has described the role Ca_i^{2+}-activated calpain remodelling of the actin cytoskeleton might play during host cell infection by CVBs [3].

We wanted therefore to understand the role of calpain during CVB1 infection and subsequent CVB1$_i$-mEV release from infected cells, as well as during virus-triggered apoptosis in target cells. To this aim we performed infection assays on HeLa cells knocked down for μ- and m-calpain isoforms using calpain small-subunit 1 small interfering RNA (*CAPNSI* siRNA). Silencing effectiveness was confirmed by immunoblotting (Fig. S3A), flow cytometry analysis (Fig. S3B and C) and immunofluorescence microscopy (Fig. S3D). Calpeptin-mediated inhibition of calpain and knockdown of CAPNS1 led to a noticeable decrease in CVB1-induced mEV release over

12 h (Fig. 1D, spotted green bars) and of CVB1-induced apoptosis within 24 h (Fig. 1E, spotted green bars) as opposed to untreated (No HPP [HiPerfect transfection reagent]) or control siRNA-treated HeLa cells. Having thus confirmed the role of calpain in mEV production and virus-elicited apoptosis, we sought to confirm the importance of calpain and associated mEV production in CVB1 infection. Notably, knockdown of CAPNS1 and calpeptin treatment (which both led to abrogation of CVB1$_i$-mEV production (Fig. 1D)), resulted in a dramatic reduction of CVB1 infection (anti-CVB1 fluorescence by flow cytometry reduced from 33% to 17.6% and 17.3%, respectively) (Fig. 1F); the immunofluorescent detection of CVB1 by microscopy was also significantly diminished (Fig. 1F). At this point however it was still not clear whether decreased CVB1 infection was due to decreased mEV release and/or other calpain-mediated processes.

Infection levels with naked CVB1 virions together with CVB1-carrying mEVs are significantly reduced with calpeptin

The enhanced levels of apoptosis measured during CVB infection cannot always be attributed to induction of apoptosis by lytic viruses [13]. Taking care, following infection, to exclude reinfection with any released free virus, apoptotic bodies or released EVs, by hourly removal of cell culture supernatants, we carried out the following experiments: essentially, we examined the possibility that CVB1$_i$-mEVs released from CVB1-infected HeLa cells (unlike mEVs constitutively released from uninfected HeLa cells [c-mEVs]), may themselves induce early apoptosis. We first carried out a time-course to monitor apoptosis levels induced by CVB1 (Fig. S4A). This showed 24.1% total apoptosis after 24 h and 56.3% after 48 h. In further experiments, we found that 24 h after incubation with CVB1$_i$-mEVs (just as with naked CVB1) the apoptosis in HeLa cells that was induced (Fig. 2A, red bars), was reduced after pre-treating cells with calpeptin (CP) (Fig. 2A, blue bars). Apoptosis of healthy cells, whether induced by CVB1 or CVB1$_i$-mEVs was also significantly reduced in the presence of the pan-caspase inhibitor, zVAD or in combination with CP (Fig. 2A, black bars).

To investigate the presence of CVB1 in mEVs, semiconfluent HeLa cells were co-cultured with CVB1 or CVB1$_i$-mEVs (red bars in Fig. 2B), the latter collected over 12 h. CVB1 and CVB1$_i$-mEVs were also added to cells pretreated with calpeptin (CP) (blue bars in Fig. 2B)). Consistency of viral load for CVB1 (MOI of 5) and CVB1$_i$-mEVs (10 EVs/cell) was estimated as follows: the infections with 10 CVB1$_i$-mEVs/cell (34% of which were estimated to be CVB1+ from electron microscopy, Fig. 3K) were thus considered equivalent to 3 CVB1 virions/cell (MOI 3.4). As a control, HeLa cells were treated with mEVs constitutively released from untreated cells (c-mEVs) or sham-infected. Every hour, after the initial infection had commenced, cell culture supernatant was removed to prevent any CVB1$_i$-mEVs, released (free) CVB1, or apoptotic bodies, from re-infecting host cells. Using immunofluorescence staining, in these CVB1$_i$-mEV-infected cells, punctate fluorescence confirmed the presence of CVB1 viral capsid antigen 30 min p.i. (Fig. S5A). The presence of CVB1 VP1 antigen 24 h p.i. (Fig. S5B) represents newly produced virions (not virus entering the cell) as reinfection was prevented by removal of medium. Representative images also show CVB1 infection 24 h p.i. (Fig. S4C), which was reduced in the presence of calpeptin (Fig. S4D). Flow cytometry analysis using anti-CVB1 Alexafluor 488, confirmed presence of virions within infected HeLa cells after 12 h co-incubation with CVB1 (~33%), or CVB1$_i$-mEVs (~22%) (Fig. 2B, red bars). Whilst neutralising anti-CVB1 was able to significantly reduce infection with naked CVB1, it had little impact on infection with mEVs from HeLa cells infected with CVB1 (CVB1$_i$-mEVs) (Fig. 2B, pink bars). Similarly, we found that CVB1$_i$-mEVs (but not CVB1) pretreated with neutralizing antibody could still also infect HeLa pretreated with increasing neutralizing antibody (Fig. S4E and C, respectively). Additionally, anti-CAR, whilst only marginally reducing infection with CVB1$_i$-mEVs, was able to block entry of naked CVB1 (Fig. 2B, green bars). Reduced anti-CVB1 staining was detected in cells pre-treated with calpeptin before co-culturing with CVB1 (15%) or CVB1$_i$-mEVs (8%) (Fig. 2B, blue bars). By contrast, no anti-CVB1-Alexafluor fluorescence was detected in sham-infected cells, or in cells co-cultured with c-mEVs (Fig. 2C, white bars). Of note, cells co-infected with CVB1 (MOI 5) and CVB1$_i$-mEVs (10 EVs/cell) stained significantly more for anti-CVB1 (~42%) (black bar) than with CVB1 alone. This suggested presence of virus in CVB1$_i$-mEVs. The anti-CVB1 fluorescence level was reduced to 18% with calpeptin pre-treatment.

11

Immunoblotting with anti-CVB1 confirmed CVB1 (VP1 protein) in CVB1$_i$-mEVs (Fig. 3A), purified by sucrose gradient. Lysates of CVB1-infected HeLa cells were also VP1-positive (Fig. 3A)., and corresponding mEVs released (Fig. 4A), were shown to carry CVB1, detected as viral capsid protein VP1, by immunoblotting with anti-CVB1. Further analysis of the same CVB1$_i$-mEVs collected 12 h p.i. also revealed the presence of activated caspase-3 (Fig. 3A), (which could also therefore be a factor in the apoptosis observed upon treatment of HeLa cells with CVB1$_i$-mEVs). Activated caspase-3 began to be detected in increasing amounts in the parent cells from 8-12 h p.i. (Fig. S6A and B) and in dexamethasone-treated, control cells and released mEVs (Fig. S6C). We also carried out hemi-nested PCR (hnPCR) on RNA complex-free sucrose gradient-purified mEVs, confirming presence of CVB1 in CVB1$_i$-mEVs released from infected cells (Fig. 3B). Electron microscopy confirmed the presence of an icosahedral viral capsid, ~30 nm in diameter, in CVB1$_i$-mEVs collected 12 h p.i. (Fig. 3C-H), but not in mEVs collected only 2 h p.i. (Fig. 3I and J). mEVs harbouring 2 or 3 virions were also observed (not shown) but none with multiple viral particles as for poliovirus [79]. Although it is likely that virions could attach to the surface of mEVs, especially where mEVs express surface virus receptors, this was not observed. To quantify the number of mEVs harbouring CVB1 virions released from CVB1-infected HeLa cells, TEM images were analysed. Five TEM fields of view (37,805× magnification) were quantified noting electron-dense virions of ~30 nm diameter as shown in Fig. 3D (60 nm EV) and F (100 nm EV). In total we found 37/108 (34%) of mEVs to harbour CVB1 (Fig. 3K). We also found that mEVs released from infected cells (CVB1$_i$-mEVs) and those constitutively released from uninfected cells (c-mEVs) had different morphologies manifest as scatter changes by flow cytometry (Fig. 3L). Specifically, CVB1$_i$-mEVs had a higher side scatter (SSC), which correlates with granularity and/or cell/EV density, than for c-mEVs, reminiscent of such changes seen in the later stages of apoptosis [80].

The data so far implied that CVB1 requires calpain activation for infection and subsequent induction of CVB1$_i$-mEVs. CVB1$_i$-mEVs carrying CVB1 virions, released by a non-lytic mechanism, are then able to deliver CVB1 to recipient cells which, *in vivo*, could thus have the potential to cause infection at secondary sites.

mEVs are taken up by CVB1-stimulated macropinocytosis in non-phagocytic, non-polarized HeLa cells and locate to late endosomes/lysosomes
To investigate whether PKH67-labelled mEVs upon CVB1-mediated uptake into the cell associate with early macropinosomes we first carried out a pulse-chase experiment using fluorescent dextran. Eight minutes after having stimulated pulse labelled Dextran-FITC HeLa cells with EV-depleted CVB1, dextran-FITC uptake was located within cells near the surface, indicating new macropinosome (MP) formation, as opposed to endosomes (Fig. 4A). By 15 min p.i., the signal indicating MPs had further increased (Fig. 4A). There was also evidence of ruffle formation (TEM in Fig. 4A) in the CVB1-stimulated cells. PKH67-mEVs in pulse labelled Dextran-Texas Red HeLa cells 15 min p.i. showed these Dextran-Texas Red MPs to contain PKH67-mEVs (Fig. 4C). Sham infected cells showed no appearance of MPs even 15 min p.i. (Fig. 4B) and no ruffle formation (Fig. 4B).

Within the cells treated with CVB1 in the presence of total EVs (30 μg), we could see by electron microscopy (Fig. S7A), large vacuoles (typically 0.2-5 μm in diameter) which were near the surface and lacking any sign of 'cell surface' structures (such as protein at the 'cytoplasmic face') and thus suggestive of macropinosomes (MPs). These MPs were found to carry vesicles ranging from 50 nm to 500 nm in diameter (Fig. S7A), and were distinct from multivesicular bodies (MVBs), 250-1000 nm in size carrying an homogenous population of intraluminal vesicles (ILVs)/sEVs (~50 nm) (Fig. S7B, C).

To ascertain the fate of endocytosed mEVs within the cytoplasm we looked at the distribution of PKH67-labelled mEVs within cells. Specifically, we looked for the PKH67-labelled mEVs at certain key structures within the cytoplasm that constitute the endocytic pathway. To this end, we focused on late endosomes and lysosomes, by using LysoTracker, a red fluorescent dye to label acidic organelles. pKH67-mEVs and Dextran-FITC in HeLa cells pulse labelled with Lysotracker (60 min p.i.) showed a partial colocalization of PKH67-mEVs with Lysotracker

CONFIDENTIAL

(Fig. 4D and quantification, r_p=0.45) and a strong colcocalization of Dextran-FITC with Lysotracker (Fig. 4E and quantification, r_p=0.58) the latter as a positive control for detection of material taken up and being located to late endosomes/lysosomes. This indicated that mEVs, following uptake by macropinocytosis, here stimulated by CVB1, in non-phagocytic HeLa cells, may follow the endosomal pathway leading to lysosomes. This is however in contrast to what has been described before in terms of a recycling fate for macropinosomes in HeLa cells [81]. This means that either a degradative or recycling pathway for mEVs taken up into MPs is likely, although what may stimulate any specific pathway, which may also depend on the MP contents, remains for now unclear.

Uptake of mEVs in epithelial cells by CVB1-stimulated macropinocytosis is inhibited by Na$^+$/H$^+$ ion exchange pump inhibitors

We first demonstrated that uptake of mEVs or Dextran could be competitively inhibited with unlabelled mEVs (Fig. 4F) or Dextran (Fig. 4G). This ruled out the possible transfer to the cells of unincorporated PKH67 or FITC label from the mEVs or dextran, respectively. Removal of surface protein from HeLa cells with trypsin also provided a partial reduction of mEV uptake (Fig. 4F) suggesting a role for protein interaction. This is unlikely to be PtdSer/PtdSer-Receptor mediated, there being a negligible reduction in mEV uptake by blocking exposed PtdSer on mEVs with unlabelled An-V (Fig. 4F). Macropinocytosis occurs in cholesterol-rich domains of the plasma membrane [82] and so as expected disruption of lipid rafts by methyl-β-cyclodextrin (MβCD), which extracts cholesterol from membranes, resulted in an almost 50% reduction in mEV uptake (Fig. 4F). Treatment with amiloride, an inhibitor of the Na$^+$/H$^+$ ion exchange pump, which affects the intracellular pH, thus blocking macropinocytosis, resulted in a 65% reduction in mEV entry (Fig. 4F). An amiloride analogue, 5-(N-ethyl-N-isopropyl)amiloride (EIPA), was slightly more potent. Inhibition of dynamin 2 GTPase with dynasore (Dyna) also reduced mEV uptake (although this inhibitor blocks clathrin- and caveolae-mediated endocytosis in HeLa [83]. Inhibition of protein kinase C, which can induce ruffling and is activated downstream of αV integrins, with the inhibitor bisindolylmaleimide (Bis), also reduced mEV uptake. In macropinocytosis, the membrane ruffling and appearance of lamellipodia or blebs is due to activation of actin and as expected we found Cytochalasin D (Cyt D) which depolymerises actin, and would therefore reduce membrane ruffling, a prerequisite for MP formation, to reduce uptake by macropinocytosis. Inhibition of microtubules with nocodazole also prevented macropinocytosis which with all the previous data, is consistent with an uptake by macropinocytosis [84], in this case of mEVs. Similar results were obtained for the uptake of Dextran-FITC (Fig. 4G). It was noted that none of the inhibitors tested had any deleterious effect on cell viability in these experiments (Fig. 4H). Interestingly, in the absence of decomplemented serum (NHS), uptake of mEVs by HeLa cells was approximately half that obtained in the presence of serum (Fig. S7D). Whether some opsonic effect on the mEVs enabling them to bind was promoting their uptake by macropinocytosis can only be conjectured upon at this stage.

mEVs from CVB1-infected HeLa cells, carrying CVB1 virions, elicit further production of mEVs, that dose-dependently induce a calpain-dependent apoptosis

Given the presence of CVB1 virions inside CVB1$_i$-mEVs, we sought to determine whether they could elicit the further release of CVB1-carrying mEVs, as did CVB1 alone. This could offer an explanation as to the role of CVB1$_i$-mEVs in the rapid dissemination of CVB1 (and likely of mEVs disseminating other non-enveloped virus pathogens) to neighbouring cells. We co-cultured HeLa cells with CVB1$_i$-mEVs isolated from CVB1-infected HeLa cells in increasing amounts or with constitutively released mEVs from unstimulated, uninfected cells (c-mEVs). As for sham-infected cells, those treated with c-mEVs, failed to induce further release of mEVs (Fig. 5A, white bars) collected after 12 h. Conversely, CVB1$_i$-mEVs stimulated a significant release of more mEVs, albeit not in a dose-dependent manner (Fig. 5A, pink bars). mEVs released from cells treated with dexamethasone (DEX), (DEX-mEVs) (Fig. 5A, green bar) which stimulated further production of mEVs were not affected by calpeptin (Fig. 5A, green spotted bar). Conversely, CVB1$_i$-mEV-elicited release of mEVs was significantly reduced when cells were pre-treated with calpeptin (Fig. 5A, spotted deep pink bar). This further suggested that the release of EVs was mediated by virus (in this case associated with the CVB1$_i$-mEV) and much less so by 'apoptotic mEVs,' (released from DEX-treated cells) which lacked virus.

13

Further analysis confirmed the induction of apoptosis in HeLa cells co-cultured with CVB1$_i$-mEVs 24 h p.i.,in a dose-dependent manner (Fig. 5B, pink bars), that was reduced upon pre-treatment with calpeptin (Fig. 5B, spotted pink bars); apoptosis in the treated HeLa cells was confirmed by detection of active caspase-3 by western blotting (Fig. 5B, inset). The CVB1$_i$-mEVs were also cytopathic as detected by plaque assay (Fig. 5C) showing cell shrinkage, rounding, cytoplasmic blebbing and detachment and at increased levels in combination with CVB1 (Fig. 5E). As expected, there was no apoptosis induced by c-mEVs from sham-infected cells. This further implies presence of CVB1 virions inside CVB1$_i$-mEVs. As with the lytic counterpart, CVB1 alone, the results show that CVB1 encapsulated within CVB1$_i$-mEVs are able to disseminate virus particles to new cells by a non-lytic mEV-to-cell mechanism. This requires calpain activation and depolymerization of the host cytoskeleton for infection and enhancement of CVB1$_i$-mEV production; furthermore, there is a reduced cytopathic effect when cells are treated with calpeptin.

Discussion

Many infectious pathogens have developed strategies to subvert host epithelial or endothelial barriers, thereby invading and spreading to secondary sites of infection. Recent studies have established that CVBs enter polarized cells, such as Caco-2 (intestinal epithelial cells) by an endocytic mechanism that at first was likened to a hybrid of macropinocytosis and caveolar-mediated endocytosis [85] and that was later shown to require the activation of specific signalling molecules including the Src family of tyrosine kinases [3, 86]. By contrast CVB3 enters non-polarised HeLa cells by clathrin-mediated endocytosis [5], later studies showing a dependence on dynamin and lipid rafts [4]. Whilst we know that spread of viral progeny to secondary sites during infection is not exclusively achieved by cell lysis [10, 11], the exact mechanism(s) remain unclear. Studies such as the demonstration of a non-lytic cell-to-cell strategy that involves CVB3 induction of cellular protrusions [13] suggested an alternative. This work showed CVB3 to translocate (in a manner sensitive to cytochalasin) through microtubule-containing cellular protrusions between green monkey kidney cells. We observed similar structures containing CVB1 between HeLa cell (Fig. S8) Whilst there is no mention of EVs, their release, in addition to the formation of membranous cellular protrusions from CVB3-infected cells, would seem likely. Indeed, close inspection of the time lapse work [13] suggests that mEV-like vesicles are released. In the later stages of CVB infection, after viral replication, to facilitate release of viral progeny, the virus induces apoptosis in infected host cells [7]. As infected cells die, virions may be found within apoptotic bodies as for adenovirus [87] which may then be distributed by phagocytosis. Work to understand the mechanism for nonlytic viral spread and how viral progeny disseminate to more distant regions to infect new cells is ongoing. This study has investigated the nonlytic mechanism of infection involving mEVs, that are released upon CVB1 infection of cells. This describes CVB1 virions encapsulated within mEVs (CVB1$_i$-mEVs) which can be disseminated (potentially to secondary sites) to infect new cells. We are further able to postulate novel ways of controlling viral cell-to-cell spread.

As we and others have reviewed, mEV release is an important mechanism, by which cells communicate and is being shown to be increasingly important in numerous disease states [24, 27, 88, 89]. Fusion of mEVs with target cells [39, 90], means they can deliver a range of intravesicular and surface molecules to recipient cells [91]. Whether virus still encapsulated within mEVs would be delivered by fusion which would mean bypassing the normal receptor (DAF and/or CAR) interactions, depending on the cell, and result in a complete viral life cycle, is not yet clear. As a precedent for mEV delivery of encapsulated virus by membrane fusion, we and others already showed likely fusion (or hemifusion) of octadecyl rhodamine labelled mEVs to cells by a lipid mixing assay [39, 92]. Following fusion of CVB1-containing mEVs with target cells, which would likely not allow for conventional viral uncoating, as would occur in an acidified endosome, mEV-delivered cytosolic CVB1 may egress rapidly within mEVs. This would occur before significant apoptosis is induced later in the viral life cycle, 24-48 h (Fig. S4A) for CVB1 and CVB3 (24-55% apoptosis; 24-42 h p.i.) [93]. Such virus-carrying mEVs may in turn themselves stimulate further mEV release.

The uptake of intact mEVs, by endocytosis [94], and delivery of surface macromolecules but also of intravesicular cargo to recipient cells has been well described [92, 95, 96]. As CVB1 virions egress infected cells there are also likely to be CVB1-containing mEVs (by uptake of nascent virus into mEVs). Mechanisms of packaging of virions into EVs, of all subtypes, varies between viruses and is still an area of much investigation. Although beyond the scope of this study, descriptions of packaging of virus in EVs still lack full mechanistic details: (i) some non-enveloped picornaviridae that are packaged in autophagosomes, are prevented from undergoing a SNARE-mediated fusion with lysosomes, instead fusing with the plasma membrane to release virus-encapsulated EVs [97-100]. (ii) Norovirus is spread within exosomes, virions being taken up into MVBs [101]. (iii) Rotavirus is shed in larger EVs released from the budding plasma membrane [101].

mEVs carrying virus may in turn be taken up by non-receptor mediated endocytosis (macropinocytosis) a process which for CVB3 and the epithelial cell tight junction protein, occludin, occurs 60-90 min p.i. [86]. Where virus is delivered by fusion of CVB1$_i$-mEVs with target cell, and not likely to be uncoated, then a nonlytic egress of non-

nascent virions in ≤ 2h, before cell lysis, and before any neighbouring cells receive apoptotic-inducing signals, would be more likely. Although the *in vivo* half-life of mEVs remains uncertain, the protection they may afford non-enveloped viruses against immune effector mechanisms is clear. If the CVB-encapsulated mEV releases virus before reaching any potential secondary site of infection, this would enable a more typical uptake by receptor-mediated endocytosis.

Recently, CVBs were reported to specifically exploit Ca^{2+}-mediated signalling events to facilitate their entry into polarized endothelial cells [3]. Using different cells, and CVB1 rather than CVB3, we found maximal increase in $[Ca^{2+}]_i$ within 100 s of cells being exposed to virus. An increase in $[Ca^{2+}]_i$ also results in a calpain-mediated depolymerization of the cytoskeleton and deimination of actin, mediated by peptidylarginine deiminases [19]. This enzymatic disassembly of the actin cytoskeleton in turn causes a release of EVs [52, 102]. This may be as a result of signal transduction initiated, at least in tumor cells, by ADP-ribosylation factor 6 [103]. We found the mechanism of CVB1-triggered mEV release to be dependent on $[Ca^{2+}]_i$, as it was sensitive to BAPTA-AM (Fig. 1A). CVB1$_i$-mEVs, themselves carrying CVB1 protein components or virions, were able to induce release of mEVs (CVB1$_i$-mEVs) (Fig. 5A) a process which could be abrogated by inhibition of calpain, using the cell-permeant calpeptin (Fig. 5A). In addition, knockdown of *CAPNS1* severely reduced CVB1 induction of mEV release and apoptosis (Fig. 1D and E, respectively). CVB1$_i$-mEVs also dose-dependently induced apoptosis in target cells that could be inhibited with calpeptin (Fig. 5B). Although CVB3-RD variant and CVB4 were shown previously [3] to release intracellular calcium in polarized endothelial cells, in a manner mediated through DAF, it would be interesting to see whether CVB1 also mediates Ca_i^{2+} release through interaction with cellular DAF [104]. However, it would be unlikely that any viral capsid residues would be exposed on the CVB1$_i$-mEV surface, to interact with DAF (as has been shown in detail for naked CVB3 [105, 106]). This data therefore implies that beyond CVB1 utilising host mEV production for its initial infection by the proposed mEV-to-cell route, released CVB1$_i$-mEVs then potentially enable further viral spread to new cells. It should be noted that the mEV-to-cell route could also be mediated by transfer of viral RNAs.

Viral dissemination via the mEV-to-cell mechanism may offer a unique advantage to the virus, over the cell-to-cell strategy. As for viruses inside cells, viral progeny inside mEVs would also be protected against host-mediated immune attack by host neutralising antibodies and complement. Furthermore, mEVs themselves able to participate in intercellular communication, could potentially deliver (non-enveloped) viruses closer to secondary sites of infection, possibly broadening the tissue tropism of such viruses, and helping establish this nonlytic mEV-to-cell means of infection. Besides polarized epithelial cells, CVBs are able to subvert polarized endothelial barriers [3]. To reach the known secondary sites of infection, the heart and CNS, on egressing the endothelium, CVBs would need to survive passage through the circulation and it would be here that the protection mEVs would afford CVBs, would be most effective. As well as facilitating rapid dissemination of virus, our results may explain the enhanced induction of apoptosis observed in neighbouring cells during CVB1 infection. At the same time, removal of activated caspase-3 from cells, in released CVB1$_i$-mEVs, is probably advantageous to the infecting CVB1, if this protects the cell from apoptosis [107] during the early phase of infection.

Just as adenovirus within apoptotic bodies may be distributed by phagocytosis [3], CVB1$_i$-mEVs, with exposed PtdSer, may also be phagocytosed and thereby distributed similarly. However, the relative contribution of the mEV-to-cell means of infection to the *in vivo* transmission of non-enveloped virus remains unknown. It was noteworthy that the level of CVB1 detected by immunofluorescence microscopy was 53% greater upon infection with CVB1 (MOI 5 or 5 PFU/cell) than CVB1$_i$-mEVs (10 EVs/cell) alone (Fig. 2B). However, with only 34% of CVB1$_i$-HeLa mEVs being CVB1$^+$ (Fig. 3K), the 10 CVB1$_i$-mEVs/cell used in infection experiments only really equated to 3 CVB1$^+$ CVB1$_i$-mEVs/cell, meaning there were ~67% more naked CVB1 virions than EV-encapsulated virions, per cell.

We found mEV uptake by epithelial cells stimulated with CVB1, to be a process dependent on lipid rafts, Na^+/H^+ ion exchanger, activation of actin, microtubules, dynamin and PKC activity, thus conducive with macropinocytosis [108]. This is a process known to be stimulated by CVB itself [109]. This is especially supported by the evidence of mEVs in MPs from confocal (and electron) microscopy, as well as that showing Dextran and labelled mEVs co-localizing to late endosomes/lysosomes. If macropinocytosis stimulated by apoptotic mimicry, whether from a microorganism, apoptotic body [61] or EVs, is dependent on PtdSer interaction with cellular receptor, then the paucity of PtdSer receptors on HeLa cells would suggest an alternative. Receptors, such as $\alpha V\beta3$, calreticulin or Axl on recipient cells could interact with PtdSer via bridge molecule(s). These may be found in serum, [110], and may include MRG-E8 (ligand for $\alpha V\beta3$), C1q (ligand for calreticulin) or protein S (ligand for Axl) [111, 112]. Indeed, we showed such a bridge molecule, protein S, to bind to mEVs released from stimulated cells, so called sMVs or s-mEVs carrying higher levels of PtdSer than those released constitutively, cMVs or c-mEVs [17]. Of note, a macropinocytosis that was serum-mediated or enhanced, as we also suggested in this study (Fig. S7D), was described for viral uptake through macropinocytosis [113] and of platelet mEVs by endothelial cells [94]. It should also be noted that PtdSer receptors as found on macrophages may in certain cases be expressed even in epithelial cells, and may also contribute to macropinocytosis, as they do to phagocytosis, in particular in the case of mammary alveolar epithelial cells. These cells, to cope with massive apoptosis during weaning of the mammary gland following lactation, have been shown to acquire phagocytic capabilities [114]. Macropinocytosis of mEVs may also be stimulated by chemokines or growth factors delivered by the mEVs themselves. Platelet-derived growth factor (PDGF) which is expressed on HeLa [115] for example stimulates macropinocytsois in fibroblasts [116]. Importantly, any specificity of uptake by macropinocytosis of mEVs is likely to be brought about by the specific combination of receptors on the recipient cell and growth factors/chemokines carried on the mEV and therefore not as unspecific as might be expected. We have demonstrated in HeLa cells, the uptake of mEVs stimulated by CVB1, to be by macropinocytosis. Whilst we have found mEVs to then locate to late endosomes/lysosomes, other potential fates, which may depend on the stimulus, and be cell-type specific, could involve recycling or maybe back-fusion with the MP membrane to still allow release of luminal contents of internalised mEVs.

It is generally accepted that many non-enveloped viruses including enteroviruses, such as CVB1, have to induce lysis of host cells in order to release progeny and spread infection [117]. mEV-to-cell transmission may be an alternative to direct cell-to-cell spread which has also been implied in another picornavirus, Ljungen virus [118] as well as the non-enveloped Rice dwarf virus, belonging to the Reoviridae, for which cell-to-cell transfer is mediated by actin-mediated protrusions [119-121]. More recently, other work showing viral transmission by a non-lytic, EV-mediated pathway has also been described [99, 122]. This study provides a platform, through modulation of mEV release, for limiting the spread of non-enveloped viruses. This will require further elucidation of pathways of mEV biogenesis which we have been actively pursuing [19, 60] leading to discovery of specific pharmacological inhibitors of mEV release [19, 60, 62, 123]. In this study we described calpeptin inhibiting infection levels of CVB1 in HeLa cells treated with CVB1, CVB1$_i$-mEVs or in combination. Calpeptin, inhibits mEV release. As non-enveloped CVB1 and other enteroviruses can be released in mEVs, inhibition of mEV release should be further studied as it likely describes another means by which calpeptin can limit viral infection. Indeed calpeptin is known to inhibit viral infections at various point of the virus life cycle [124-126].

Finally, as we recently reviewed, we are now moving into an era that will see the development of EV-based drug delivery systems [15, 127]. However, as this study and others have highlighted, mEVs may themselves be potential carriers of deliverable non-enveloped viruses. Such information will become increasingly important as new quality control measures are drawn up for the transition of EV-based therapies into the clinic.

Author Contributions

S.J. and E.A.A. performed the experiments, contributed to data analysis and discussions and helped write the manuscript. K.M., B.B., M.L. and P.W. contributed to some experiments. S.L., K.M., D.S., B.B., M.L. and A.S. contributed to data analysis and discussions. J.M.I contributed to experimentation, data analysis, discussions, wrote the paper, conceived, supervised and financed the project.

Conflict of interest

The authors declare no competing financial interests.

Figure Legends

Fig. 1 CVB1 infection and CVB1-mediated mEV release and apoptosis of HeLa cells is inhibited upon downregulation of calpain (A), Semi-confluent HeLa cells were infected with CVB1 (MOI 5) for 1 h; after washing, cells were resuspended in serum-free medium for 2 h or 12 h, having been pre-treated or not with calpeptin (CP) or BAPTA-AM (both at 20 μM, 37 °C for 45 min) for 1 h. Where mEV release was monitored over 12 h, supernatants were collected hourly, to minimise the chance of any released mEVs or virus from interacting with the infected cells. mEVs (in the 50 to 650 nm diameter size range) were quantified by Nanosight Tracking Analysis (NTA). BAPTA-AM, which abrogated mEV release did not induce apoptosis (AnV$^+$/7-AAD$^+$) (B), nor induce permeabilization (no PI fluorescence) (C). Intracellular calcium was monitored using Fura-2-AM in HeLa cells infected with CVB1 over 2.5 min (C). In (D), sham-infected HeLa cells ('Sham' or 'No HPP') or siRNA-treated cells (to downregulate calpain) or calpeptin pre-treated cells were co-cultured with CVB1 (MOI 5) for 12 h and released CVB1$_i$-mEVs isolated and quantified by NTA. (E), to analyse the effect of calpain knockdown on virus-induced early apoptosis, siRNA-treated HeLa cells infected with CVB1 were assessed for staining with AnV-FITC by flow cytometry after 24 h. Data presented is the mean ± SD of three separate experiments performed in triplicate. ** *P*< 0.01 and *** *P*< 0.001 were considered statistically significant using Student's *t*-test. (F), Flow cytometry analysis of intracellular CVB1 (12 h) after siRNA or calpeptin treatment of HeLa cells to knock down expression or inhibit calpain. Sham-infected cells or *CAPNS1* siRNA-treated HeLa cells infected with CVB1 were fixed and permeabilised prior to staining with anti-CVB1 conjugated with Alexafluor 488-IgG antibody. Representative data are of two independent experiments performed in triplicate. Immunostaining of CVB1 inside infected HeLa cells after siRNA treatment for 12 h or calpeptin pre-treatment (20 μM/45 min/37 °C), as assessed by fluorescent microscopy.

Fig. 2 Target cell infection and apoptosis induced by CVB1-infected HeLa mEVs (CVB1$_i$-mEVs) can be reduced by modulation of calpain (A), Early apoptosis of HeLa cells (AnV-FITC$^+$) after 12 h, induced by CVB1 particles (MOI 5) or CVB1-induced HeLa mEVs collected at t=12 h (10 CVB1$_i$-mEVs per cell), both in presence or absence of calpeptin (cells pre-incubated with 20 μM for 45 min at 37 °C) and/or the pan-caspase inhibitor zVAD (pre-incubated with 20 μM for 30 min at 37 °C). HeLa c-mEVs (constitutively released mEVs from uninfected cells) collected after 24 h, were also added as a control. (B), Flow cytometry analysis of intracellular CVB1 fluorescence after co-culture of CVB1 particles (MOI 5) with HeLa cells for 12 h, or co-incubation with mEVs from various cells (from non-infected cells [c-mEVs, constitutively released] or from infected cells collected at t=12 h [CVB1$_i$-mEVs]; 10 mEVs/cell). To monitor the effect of calpeptin, cells were pre-treated (as for apoptosis experiments in (A)), prior to addition of CVB1 particles or CVB1$_i$-mEVs and incubated at 37 °C for 12 h. Where necessary, cells were also treated with a 1:50 dilution of blocking anti-CAR antibody (20 μg/ml) or isotype control, 90 min before introducing CVB1. CVB1 or CVB1$_i$-mEVs were also incubated for 90 min before infection with neutralising anti-CVB1 antibodies (62.5 μg/ml, see Materials and Methods). Data presented is the mean ± SEM of three independent experiments performed in triplicate. **P <0.01, ***P <0.001 were considered statistically significant.

Fig. 3 CVB1$_i$-mEVs carry the non-enveloped Coxsackie virus B1 (A), western blotting analysis of HeLa cell or mEV lysates (purified through a sucrose gradient) isolated from sham-infected (-) or CVB1-infected (+) cells after 12 h. As loading controls, cellular proteins were probed with anti-β-actin (1/500) and for EVs, total proteins analysed determined by staining with MemCode. Proteins were probed with anti-CVB1, anti-procaspase-3 and anti-active procaspase-3 (all at 1/500). (B), hemi-nested PCR was carried out to reveal CVB1 RNA within mEVs released from infected cells (CVB1$_i$-mEVs) after 12 h, but not c-mEVs (constitutively released mEVs) released from non-infected cells. Transmission electron microscopy (TEM) (C-J), was performed on CVB1$_i$-mEVs, collected 12 h p.i., to reveal an electron dense viral capsid (~30 nm in diameter). White arrows indicate viral capsid detected within an mEV, the black arrow shows a virus-free mEV and the red asterisks indicate non-encapsulated virus. mEVs isolated from conditioned medium of infected HeLa cells after 2 h (I and J) reveal no sign of viral capsids. (K), Analysis of 5 TEM fields (37,805× magnification) of released mEVs from CVB1-infected HeLa revealed

19

34% of mEVs harbouring CVB1. (L), Forward/side scatter dot plots for mEVs released from CVB1-infected HeLa cells (CVB1$_i$-mEVs) or constitutively released from uninfected cells (HeLa c-mEVs).

Fig. 4 Uptake of PKH67-labelled mEVs by CVB1-stimulated macropinocytosis in HeLa cells
Cells stimulated with CVB1 (30 μg) showed the appearance of macropinosomes (MPs) (Dextran-FITC containing vacuoles near the cell surface) within 8 min p.i. and with increased numbers by 15 min p.i., (A). CVB1 stimulation also resulted in a ruffled appearance on the cell surface with protrusions of lamellipodia, 15 min p.i., (A). By contrast, sham infected HeLa showed no Dextran-FITC MPs and no ruffled appearance of the cell surface (B). To locate PKH67-labelled mEVs after 15 min endocytosis, cells were co-labelled with Dextran-Texas Red to identify macropinososomes (MPs) (C). Confocal analysis was used 60 min after endocytosis of mEVs to ascertain whether PKH67-mEVs as well as Dextran-FITC (as a positive control for uptake by macropinocytosis) co-localize with late endosomes/lysosomes using Lysotracker. This indeed showed co-localization of both PKH67 mEVs (D) and Dextran-FITC (E) with late endosomes/lysosomes after 60 min. Colocalization between either PKH67-mEVs or Dextran-FITC and LysoTracker was quantified using 25 cells to calculate the Pearson's colocalization coefficient, r_p. Uptake of PKH67-mEVs (after pre-stimulation with mEV-depleted CVB1) or of Dextran-FITC was monitored by flow cytometry in the presence of potent inhibitors of macropinocytosis, MβCD, amiloride, EIPA, dynasore, bisindolylmaleimide, cytochalisin D and nocodozole, (F and G). The effect of protein removal (using trypsin) from the acceptor cell was also monitored as was the effect of blocking phosphatidylserine with An-V, (F and G). Percentage viability was maintained throughout (H). The data represent the mean ± S.E.M. for three independent experiments (ns, not significant; *P<0.05, **P<0.01, ***P<0.001).

Fig. 5 HeLa cells treated with CVB1$_i$-mEVs elicit a further release of CVB1$_i$-mEVs able to induce apoptosis in target cells (A), HeLa cells were treated with CVB1-induced HeLa mEVs (CVB1$_i$-mEVs), in increasing amounts (1, 5 and 10 mEVs/cell), for 12 h and as a control with mEVs constitutively released from semi-confluent uninfected cells (c-mEVs); mEVs from HeLa cells treated for 12 h with 1 mM dexamethasone (DEX-mEVs) (or 'apoptotic mEVs,' (a-mEVs)) were also added with or without calpeptin (CP). CVB1-infected HeLa cells (at MOI 5) were also included for comparison of mEV release (CVB1 gave a 67 % increased level of mEV release from HeLa cells compared to CVB1$_i$-mEVs (at 10 mEVs/cell)). (B), Flow cytometry analysis of early apoptosis in sham-infected HeLa cells or HeLa co-cultured with c-mEVs or HeLa cell-derived CVB1$_i$-mEVs (1, 5 and 10 mEVs/cell) in presence or absence of calpeptin (CP) after 24 h at 37 °C. mEVs from DEX-treated (1 mM for 12 h) HeLa cells were also added to show induction of apoptosis of target cells. Apoptosis levels induced from CVB1-infected HeLa cells (at MOI 5) was also included for comparison (giving a 40% increased level of apoptosis compared to CVB1$_i$-mEVs (at 10 mEVs/cell)). Apoptosis was assessed by staining with AnV-FITC and 7-AAD according to the manufacturer's instructions. Western blotting (inset) shows detection of activated caspase-3 upon addition of 10 CVB1$_i$-mEVs/cell but not in the presence of calpeptin. Data represents the mean ± SD of two separate experiments performed in triplicate. **P <0.01, ***P <0.001 were considered statistically significant. (C-H) Microscopy images of HeLa cells infected with CVB1$_i$-mEVs (10 mEVs/cell), or CVB1 (MOI 5) in the presence or absence of calpeptin after 24 h. Scale bar = 100 μm. Images are representative of duplicate experiments performed in triplicate.

References

1.   **Tracy S, Gauntt C**. Group B coxsackievirus virulence. *Curr Top Microbiol Immunol* 2008;323:49-63.
2.   **Romero JR, Selvarangan R**. The human Parechoviruses: an overview. *Adv Pediatr* 2011;58(1):65-85.
3.   **Bozym RA, Morosky SA, Kim KS, Cherry S, Coyne CB**. Release of intracellular calcium stores facilitates coxsackievirus entry into polarized endothelial cells. *PLoS pathogens* 2010;6(10):e1001135.
4.   **Patel KP, Coyne CB, Bergelson JM**. Dynamin- and lipid raft-dependent entry of decay-accelerating factor (DAF)-binding and non-DAF-binding coxsackieviruses into nonpolarized cells. *J Virol* 2009;83(21):11064-11077.
5.   **Chung SK, Kim JY, Kim IB, Park SI, Paek KH et al.** Internalization and trafficking mechanisms of coxsackievirus B3 in HeLa cells. *Virology* 2005;333(1):31-40.
6.   **Salako MA, Carter MJ, Kass GE**. Coxsackievirus protein 2BC blocks host cell apoptosis by inhibiting caspase-3. *The Journal of biological chemistry* 2006;281(24):16296-16304.
7.   **Carthy CM, Yanagawa B, Luo H, Granville DJ, Yang D et al.** Bcl-2 and Bcl-xL overexpression inhibits cytochrome c release, activation of multiple caspases, and virus release following coxsackievirus B3 infection. *Virology* 2003;313(1):147-157.
8.   **Vuorinen T, Peri P, Vainionpaa R**. Measles virus induces apoptosis in uninfected bystander T cells and leads to granzyme B and caspase activation in peripheral blood mononuclear cell cultures. *Eur J Clin Invest* 2003;33(5):434-442.
9.   **Cheeran MC, Lokensgard JR, Schleiss MR**. Neuropathogenesis of congenital cytomegalovirus infection: disease mechanisms and prospects for intervention. *Clin Microbiol Rev* 2009;22(1):99-126, Table of Contents.
10.   **Mena I, Perry CM, Harkins S, Rodriguez F, Gebhard J et al.** The role of B lymphocytes in coxsackievirus B3 infection. *The American journal of pathology* 1999;155(4):1205-1215.
11.   **DeBiasi RL, Edelstein CL, Sherry B, Tyler KL**. Calpain inhibition protects against virus-induced apoptotic myocardial injury. *J Virol* 2001;75(1):351-361.
12.   **Ponnuraj EM, John TJ, Levin MJ, Simoes EA**. Cell-to-cell spread of poliovirus in the spinal cord of bonnet monkeys (Macaca radiata). *J Gen Virol* 1998;79 (Pt 10):2393-2403.
13.   **Paloheimo O, Ihalainen TO, Tauriainen S, Valilehto O, Kirjavainen S et al.** Coxsackievirus B3-induced cellular protrusions: structural characteristics and functional competence. *J Virol* 2011;85(13):6714-6724.
14.   **Kowal J, Arras G, Colombo M, Jouve M, Morath JP et al.** Proteomic comparison defines novel markers to characterize heterogeneous populations of extracellular vesicle subtypes. *Proceedings of the National Academy of Sciences of the United States of America* 2016;113(8):E968-977.
15.   **Moore C, Kosgodage U, Lange S, Inal JM**. The emerging role of exosome and microvesicle- (EMV-) based cancer therapeutics and immunotherapy. *International journal of cancer* 2017.
16.   **Menck K, Sönmezer C, Worst TS, Schulz M, Dihazi GH et al.** Neutral sphingomyelinases control extracellular vesicles budding from the plasma membrane. *Journal of extracellular vesicles* 2017;6(1):1378056.
17.   **Stratton D, Moore C, Antwi-Baffour S, Lange S, Inal J**. Microvesicles released constitutively from prostate cancer cells differ biochemically and functionally to stimulated microvesicles released through sublytic C5b-9. *Biochemical and biophysical research communications* 2015;460(3):589-595.

18.   **Stachowiak JC, Brodsky FM, Miller EA**. A cost-benefit analysis of the physical mechanisms of membrane curvature. *Nature cell biology* 2013;15(9):1019-1027.
19.   **Kholia S, Jorfi S, Thompson PR, Causey CP, Nicholas AP et al.** A novel role for peptidylarginine deiminases in microvesicle release reveals therapeutic potential of PAD inhibition in sensitizing prostate cancer cells to chemotherapy. *Journal of extracellular vesicles* 2015;4:26192.
20.   **Wilson KF, Erickson JW, Antonyak MA, Cerione RA**. Rho GTPases and their roles in cancer metabolism. *Trends Mol Med* 2013;19(2):74-82.
21.   **Sedgwick AE, Clancy JW, Olivia Balmert M, D'Souza-Schorey C**. Extracellular microvesicles and invadopodia mediate non-overlapping modes of tumor cell invasion. *Scientific reports* 2015;5:14748.
22.   **Schlienger S, Campbell S, Claing A**. ARF1 regulates the Rho/MLC pathway to control EGF-dependent breast cancer cell invasion. *Molecular biology of the cell* 2014;25(1):17-29.
23.   **Liao CF, Lin SH, Chen HC, Tai CJ, Chang CC et al.** CSE1L, a novel microvesicle membrane protein, mediates Ras-triggered microvesicle generation and metastasis of tumor cells. *Mol Med* 2012;18:1269-1280.
24.   **Inal JM, Ansa-Addo EA, Stratton D, Kholia S, Antwi-Baffour SS et al.** Microvesicles in health and disease. *Archivum immunologiae et therapiae experimentalis* 2012;60(2):107-121.
25.   **De Sousa KP, Rossi I, Abdullahi M, Ramirez MI, Stratton D et al.** Isolation and characterization of extracellular vesicles and future directions in diagnosis and therapy. *Wiley interdisciplinary reviews Nanomedicine and nanobiotechnology* 2023;15(1):e1835.
26.   **Pegtel DM, Peferoen L, Amor S**. Extracellular vesicles as modulators of cell-to-cell communication in the healthy and diseased brain. *Philos Trans R Soc Lond B Biol Sci* 2014;369(1652).
27.   **Lange S, Gallagher M, Kholia S, Kosgodage US, Hristova M et al.** Peptidylarginine Deiminases-Roles in Cancer and Neurodegeneration and Possible Avenues for Therapeutic Intervention via Modulation of Exosome and Microvesicle (EMV) Release? *International journal of molecular sciences* 2017;18(6).
28.   **Jorfi S, Ansa-Addo EA, Kholia S, Stratton D, Valley S et al.** Inhibition of microvesiculation sensitizes prostate cancer cells to chemotherapy and reduces docetaxel dose required to limit tumor growth in vivo. *Scientific reports* 2015;5:13006.
29.   **Muralidharan-Chari V, Kohan HG, Asimakopoulos AG, Sudha T, Sell S et al.** Microvesicle removal of anticancer drugs contributes to drug resistance in human pancreatic cancer cells. *Oncotarget* 2016;7(31):50365-50379.
30.   **Aubertin K, Silva AK, Luciani N, Espinosa A, Djemat A et al.** Massive release of extracellular vesicles from cancer cells after photodynamic treatment or chemotherapy. *Scientific reports* 2016;6:35376.
31.   **Antwi-Baffour S, Kholia S, Aryee YK, Ansa-Addo EA, Stratton D et al.** Human plasma membrane-derived vesicles inhibit the phagocytosis of apoptotic cells--possible role in SLE. *Biochemical and biophysical research communications* 2010;398(2):278-283.
32.   **Shao WH, Cohen PL**. Disturbances of apoptotic cell clearance in systemic lupus erythematosus. *Arthritis Res Ther* 2011;13(1):202.
33.   **Valenti R, Huber V, Iero M, Filipazzi P, Parmiani G et al.** Tumor-released microvesicles as vehicles of immunosuppression. *Cancer research* 2007;67(7):2912-2915.
34.   **Becker A, Thakur BK, Weiss JM, Kim HS, Peinado H et al.** Extracellular Vesicles in Cancer: Cell-to-Cell Mediators of Metastasis. *Cancer Cell* 2016;30(6):836-848.
35.   **Peinado H, Zhang H, Matei IR, Costa-Silva B, Hoshino A et al.** Pre-metastatic niches: organ-specific homes for metastases. *Nat Rev Cancer* 2017;17(5):302-317.

36.   **Jorfi S, Inal JM**. The role of microvesicles in cancer progression and drug resistance. *Biochem Soc Trans* 2013;41(1):293-298.

37.   **Robbins PD, Dorronsoro A, Booker CN**. Regulation of chronic inflammatory and immune processes by extracellular vesicles. *J Clin Invest* 2016;126(4):1173-1180.

38.   **Sarkar A, Mitra S, Mehta S, Raices R, Wewers MD**. Monocyte derived microvesicles deliver a cell death message via encapsulated caspase-1. *PloS one* 2009;4(9):e7140.

39.   **Ansa-Addo EA, Lange S, Stratton D, Antwi-Baffour S, Cestari I et al.** Human plasma membrane-derived vesicles halt proliferation and induce differentiation of THP-1 acute monocytic leukemia cells. *Journal of immunology (Baltimore, Md : 1950)* 2010;185(9):5236-5246.

40.   **Ismail N, Wang Y, Dakhlallah D, Moldovan L, Agarwal K et al.** Macrophage microvesicles induce macrophage differentiation and miR-223 transfer. *Blood* 2013;121(6):984-995.

41.   **Coakley G, Maizels RM, Buck AH**. Exosomes and Other Extracellular Vesicles: The New Communicators in Parasite Infections. *Trends Parasitol* 2015;31(10):477-489.

42.   **Cestari I, Ansa-Addo E, Deolindo P, Inal JM, Ramirez MI**. Trypanosoma cruzi immune evasion mediated by host cell-derived microvesicles. *Journal of immunology (Baltimore, Md : 1950)* 2012;188(4):1942-1952.

43.   **Antwi-Baffour S, Malibha-Pinchbeck M, Stratton D, Jorfi S, Lange S et al.** Plasma mEV levels in Ghanain malaria patients with low parasitaemia are higher than those of healthy controls, raising the potential for parasite markers in mEVs as diagnostic targets. *Journal of extracellular vesicles* 2020;9(1):1697124.

44.   **Lee Y, El Andaloussi S, Wood MJ**. Exosomes and microvesicles: extracellular vesicles for genetic information transfer and gene therapy. *Hum Mol Genet* 2012;21(R1):R125-134.

45.   **Stratton D, Moore C, Zheng L, Lange S, Inal J**. Prostate cancer cells stimulated by calcium-mediated activation of protein kinase C undergo a refractory period before re-releasing calcium-bearing microvesicles. *Biochemical and biophysical research communications* 2015;460(3):511-517.

46.   **Inal JM, Ansa-Addo EA, Lange S**. Interplay of host-pathogen microvesicles and their role in infectious disease. *Biochem Soc Trans* 2013;41(1):258-262.

47.   **Rossi IV, Nunes MAF, Sabatke B, Ribas HT, Winnischofer SMB et al.** An induced population of Trypanosoma cruzi epimastigotes more resistant to complement lysis promotes a phenotype with greater differentiation, invasiveness, and release of extracellular vesicles. *Frontiers in cellular and infection microbiology* 2022;12:1046681.

48.   **Evans-Osses I, Mojoli A, Monguio-Tortajada M, Marcilla A, Aran V et al.** Microvesicles released from Giardia intestinalis disturb host-pathogen response in vitro. *European journal of cell biology* 2017;96(2):131-142.

49.   **Badorff C, Berkely N, Mehrotra S, Talhouk JW, Rhoads RE et al.** Enteroviral protease 2A directly cleaves dystrophin and is inhibited by a dystrophin-based substrate analogue. *The Journal of biological chemistry* 2000;275(15):11191-11197.

50.   **Seipelt J, Liebig HD, Sommergruber W, Gerner C, Kuechler E**. 2A proteinase of human rhinovirus cleaves cytokeratin 8 in infected HeLa cells. *The Journal of biological chemistry* 2000;275(26):20084-20089.

51.   **Xiong D, Lee GH, Badorff C, Dorner A, Lee S et al.** Dystrophin deficiency markedly increases enterovirus-induced cardiomyopathy: a genetic predisposition to viral heart disease. *Nat Med* 2002;8(8):872-877.

52.   **Fox JE, Austin CD, Boyles JK, Steffen PK**. Role of the membrane skeleton in preventing the shedding of procoagulant-rich microvesicles from the platelet plasma membrane. *The Journal of cell biology* 1990;111(2):483-493.

53.   **Muralidharan-Chari V, Clancy JW, Sedgwick A, D'Souza-Schorey C**. Microvesicles: mediators of extracellular communication during cancer progression. *Journal of cell science* 2010;123(Pt 10):1603-1611.

54.   **Masi G, Mercati D, Vannuccini E, Paccagnini E, Riparbelli MG et al.** p66Shc regulates vesicle-mediated secretion in mast cells by affecting F-actin dynamics. *J Leukoc Biol* 2014;95(2):285-292.

55.   **Huber V, Fais S, Iero M, Lugini L, Canese P et al.** Human colorectal cancer cells induce T-cell death through release of proapoptotic microvesicles: role in immune escape. *Gastroenterology* 2005;128(7):1796-1804.

56.   **Andreola G, Rivoltini L, Castelli C, Huber V, Perego P et al.** Induction of lymphocyte apoptosis by tumor cell secretion of FasL-bearing microvesicles. *The Journal of experimental medicine* 2002;195(10):1303-1316.

57.   **Jorfi S, Ansa-Addo, E., Inal, J.M.** *Coxsackie virus entry and spread in HeLa cells is aided by microvesicle release*. 2012: The Journal of Immunology 188 (1 Supplement) 170.22; 2012.

58.   **Jorfi S, Ansa-Addo, E., Inal, J.M.** Plasma membrane-derived vesicles (PMVs) released from infected HeLa cells by Coxsackie virus B1 induce apoptosis in recipient viable cells. *Immunology 131, (Suppl 1) 222* 2010.

59.   **Inal JM, Jorfi S**. Coxsackievirus B transmission and possible new roles for extracellular vesicles. *Biochem Soc Trans* 2013;41(1):299-302.

60.   **Kosgodage US, Trindade RP, Thompson PR, Inal JM, Lange S**. Chloramidine/Bisindolylmaleimide-I-Mediated Inhibition of Exosome and Microvesicle Release and Enhanced Efficacy of Cancer Chemotherapy. *International journal of molecular sciences* 2017;18(5).

61.   **Théry C, Witwer KW, Aikawa E, Alcaraz MJ, Anderson JD et al.** Minimal information for studies of extracellular vesicles 2018 (MISEV2018): a position statement of the International Society for Extracellular Vesicles and update of the MISEV2014 guidelines. *Journal of extracellular vesicles* 2018;7(1):1535750.

62.   **Kosgodage US, Uysal-Onganer P, MacLatchy A, Mould R, Nunn AV et al.** Cannabidiol Affects Extracellular Vesicle Release, miR21 and miR126, and Reduces Prohibitin Protein in Glioblastoma Multiforme Cells. *Translational oncology* 2019;12(3):513--522.

63.   **Hui KM, Orriss GL, Schirmer T, Magnadottir B, Schifferli JA et al.** Expression of functional recombinant von Willebrand factor-A domain from human complement C2: a potential binding site for C4 and CRIT. *Biochem J* 2005;389(Pt 3):863-868.

64.   **Schindelin J, Arganda-Carreras I, Frise E, Kaynig V, Longair M et al.** Fiji: an open-source platform for biological-image analysis. *Nature methods* 2012;9(7):676-682.

65.   **Commisso C, Flinn RJ, Bar-Sagi D**. Determining the macropinocytic index of cells through a quantitative image-based assay. *Nature protocols* 2014;9(1):182-192.

66.   **Wang JT, Teasdale RD, Liebl D**. Macropinosome quantitation assay. *MethodsX* 2014;1:36-41.

67.   **Manders EM, Stap J, Brakenhoff GJ, van Driel R, Aten JA**. Dynamics of three-dimensional replication patterns during the S-phase, analysed by double labelling of DNA and confocal microscopy. *Journal of cell science* 1992;103 (Pt 3):857-862.

68.   **Bolte S, Cordelières FP**. A guided tour into subcellular colocalization analysis in light microscopy. *Journal of microscopy* 2006;224(Pt 3):213-232.

69.   **Stratton D, Lange S, Inal JM**. Pulsed extremely low-frequency magnetic fields stimulate microvesicle release from human monocytic leukaemia cells. *Biochemical and biophysical research communications* 2013;430(2):470-475.

70.   **Evans-Osses I, Mojoli A, Monguió-Tortajada M, Marcilla A, Aran V et al.** Microvesicles released from Giardia intestinalis disturb host-pathogen response in vitro. *European journal of cell biology* 2017;96(2):131-142.

71.   **O'Neill CP, Gilligan KE, Dwyer RM**. Role of Extracellular Vesicles (EVs) in Cell Stress Response and Resistance to Cancer Therapy. *Cancers* 2019;11(2).

72.   **Bernimoulin M, Waters EK, Foy M, Steele BM, Sullivan M et al.** Differential stimulation of monocytic cells results in distinct populations of microparticles. *J Thromb Haemost* 2009;7(6):1019-1028.

73.   **Durcin M, Fleury A, Taillebois E, Hilairet G, Krupova Z et al.** Characterisation of adipocyte-derived extracellular vesicle subtypes identifies distinct protein and lipid signatures for large and small extracellular vesicles. *Journal of extracellular vesicles* 2017;6(1):1305677.

74.   **Xiao X, Yu S, Li S, Wu J, Ma R et al.** Exosomes: decreased sensitivity of lung cancer A549 cells to cisplatin. *PloS one* 2014;9(2):e89534.

75.   **Le M, Fernandez-Palomo C, McNeill FE, Seymour CB, Rainbow AJ et al.** Exosomes are released by bystander cells exposed to radiation-induced biophoton signals: Reconciling the mechanisms mediating the bystander effect. *PloS one* 2017;12(3):e0173685.

76.   **Angeloni NL, McMahon KM, Swaminathan S, Plebanek MP, Osman I et al.** Pathways for Modulating Exosome Lipids Identified By High-Density Lipoprotein-Like Nanoparticle Binding to Scavenger Receptor Type B-1. *Scientific reports* 2016;6:22915.

77.   **Debiasi RL, Squier MK, Pike B, Wynes M, Dermody TS et al.** Reovirus-induced apoptosis is preceded by increased cellular calpain activity and is blocked by calpain inhibitors. *J Virol* 1999;73(1):695-701.

78.   **Bozym RA, Patel K, White C, Cheung KH, Bergelson JM et al.** Calcium signals and calpain-dependent necrosis are essential for release of coxsackievirus B from polarized intestinal epithelial cells. *Molecular biology of the cell* 2011;22(17):3010-3021.

79.   **Kim D-K, Lee J, Kim SR, Choi D-S, Yoon YJ et al.** EVpedia: a community web portal for extracellular vesicles research. *Bioinformatics* 2015;31(6):933-939.

80.   **Elstein KH, Zucker RM**. Comparison of cellular and nuclear flow cytometric techniques for discriminating apoptotic subpopulations. *Experimental cell research* 1994;211(2):322-331.

81.   **Tisdale EJ, Shisheva A, Artalejo CR**. Overexpression of atypical protein kinase C in HeLa cells facilitates macropinocytosis via Src activation. *Cellular signalling* 2014;26(6):1235-1242.

82.   **Grimmer S, van Deurs B, Sandvig K**. Membrane ruffling and macropinocytosis in A431 cells require cholesterol. *Journal of cell science* 2002;115(Pt 14):2953-2962.

83.   **Cao H, Chen J, Awoniyi M, Henley JR, McNiven MA**. Dynamin 2 mediates fluid-phase micropinocytosis in epithelial cells. *Journal of cell science* 2007;120(Pt 23):4167-4177.

84.   **Preta G, Cronin JG, Sheldon IM**. Dynasore - not just a dynamin inhibitor. *Cell communication and signaling : CCS* 2015;13:24.

85.   **Coyne CB, Bergelson JM**. Virus-induced Abl and Fyn kinase signals permit coxsackievirus entry through epithelial tight junctions. *Cell* 2006;124(1):119-131.

86.   **Coyne CB, Kim KS, Bergelson JM**. Poliovirus entry into human brain microvascular cells requires receptor-induced activation of SHP-2. *Embo j* 2007;26(17):4016-4028.

87.   **Mi J, Li ZY, Ni S, Steinwaerder D, Lieber A**. Induced apoptosis supports spread of adenovirus vectors in tumors. *Hum Gene Ther* 2001;12(10):1343-1352.

88.   **Inal JM, Kosgodage U, Azam S, Stratton D, Antwi-Baffour S et al.** Blood/plasma secretome and microvesicles. *Biochimica et biophysica acta* 2013;1834(11):2317-2325.

89.   **Arenaccio C, Federico M**. The Multifaceted Functions of Exosomes in Health and Disease: An Overview. *Adv Exp Med Biol* 2017;998:3-19.

90.   **Prada I, Meldolesi J**. Binding and Fusion of Extracellular Vesicles to the Plasma Membrane of Their Cell Targets. *International journal of molecular sciences* 2016;17(8).

91.   **Raposo G, Stoorvogel W**. Extracellular vesicles: exosomes, microvesicles, and friends. *The Journal of cell biology* 2013;200(4):373-383.

92.   **Taylor DD, Gercel-Taylor C**. The origin, function, and diagnostic potential of RNA within extracellular vesicles present in human biological fluids. *Front Genet* 2013;4:142.

93.   **Yuan JP, Zhao W, Wang HT, Wu KY, Li T et al.** Coxsackievirus B3-induced apoptosis and caspase-3. *Cell research* 2003;13(3):203-209.

94.   **Faille D, El-Assaad F, Mitchell AJ, Alessi MC, Chimini G et al.** Endocytosis and intracellular processing of platelet microparticles by brain endothelial cells. *J Cell Mol Med* 2012;16(8):1731-1738.

95.   **Kanada M, Bachmann MH, Hardy JW, Frimannson DO, Bronsart L et al.** Differential fates of biomolecules delivered to target cells via extracellular vesicles. *Proceedings of the National Academy of Sciences of the United States of America* 2015;112(12):E1433-1442.

96.   **French KC, Antonyak MA, Cerione RA**. Extracellular vesicle docking at the cellular port: Extracellular vesicle binding and uptake. *Semin Cell Dev Biol* 2017;67:48-55.

97.   **Too IH, Yeo H, Sessions OM, Yan B, Libau EA et al.** Enterovirus 71 infection of motor neuron-like NSC-34 cells undergoes a non-lytic exit pathway. *Scientific reports* 2016;6:36983.

98.   **van der Grein SG, Defourny KAY, Rabouw HH, Galiveti CR, Langereis MA et al.** Picornavirus infection induces temporal release of multiple extracellular vesicle subsets that differ in molecular composition and infectious potential. *PLoS pathogens* 2019;15(2):e1007594.

99.   **Robinson SM, Tsueng G, Sin J, Mangale V, Rahawi S et al.** Coxsackievirus B exits the host cell in shed microvesicles displaying autophagosomal markers. *PLoS pathogens* 2014;10(4):e1004045.

100.   **Chen YH, Du W, Hagemeijer MC, Takvorian PM, Pau C et al.** Phosphatidylserine vesicles enable efficient en bloc transmission of enteroviruses. *Cell* 2015;160(4):619-630.

101.   **Santiana M, Ghosh S, Ho BA, Rajasekaran V, Du WL et al.** Vesicle-Cloaked Virus Clusters Are Optimal Units for Inter-organismal Viral Transmission. *Cell host & microbe* 2018;24(2):208-220.e208.

102.   **Kalra H, Drummen GP, Mathivanan S**. Focus on Extracellular Vesicles: Introducing the Next Small Big Thing. *International journal of molecular sciences* 2016;17(2):170.

103.   **Muralidharan-Chari V, Clancy J, Plou C, Romao M, Chavrier P et al.** ARF6-regulated shedding of tumor cell-derived plasma membrane microvesicles. *Current biology : CB* 2009;19(22):1875-1885.

104.   **Spiller OB, Goodfellow IG, Evans DJ, Hinchliffe SJ, Morgan BP**. Coxsackie B viruses that use human DAF as a receptor infect pig cells via pig CAR and do not use pig DAF. *J Gen Virol* 2002;83(Pt 1):45-52.

105.   **Pan J, Zhang L, Organtini LJ, Hafenstein S, Bergelson JM**. Specificity of coxsackievirus B3 interaction with human, but not murine, decay-accelerating factor: replacement of a single residue within short consensus repeat 2 prevents virus attachment. *J Virol* 2015;89(2):1324-1328.

106.   **Pan J, Narayanan B, Shah S, Yoder JD, Cifuente JO et al.** Single amino acid changes in the virus capsid permit coxsackievirus B3 to bind decay-accelerating factor. *J Virol* 2011;85(14):7436-7443.

107.   **Böing AN, Stap J, Hau CM, Afink GB, Ris-Stalpers C et al.** Active caspase-3 is removed from cells by release of caspase-3-enriched vesicles. *Biochimica et biophysica acta* 2013;1833(8):1844-1852.

108.   **Li H, Pauza CD**. Rapamycin increases the yield and effector function of human gammadelta T cells stimulated in vitro. *Cancer Immunol Immunother* 2011;60(3):361-370.

109.   **Coyne CB, Shen L, Turner JR, Bergelson JM**. Coxsackievirus entry across epithelial tight junctions requires occludin and the small GTPases Rab34 and Rab5. *Cell host & microbe* 2007;2(3):181-192.

110.   **Korns D, Frasch SC, Fernandez-Boyanapalli R, Henson PM, Bratton DL**. Modulation of macrophage efferocytosis in inflammation. *Frontiers in immunology* 2011;2:57.

111.   **Ogden CA, deCathelineau A, Hoffmann PR, Bratton D, Ghebrehiwet B et al.** C1q and mannose binding lectin engagement of cell surface calreticulin and CD91 initiates macropinocytosis and uptake of apoptotic cells. *The Journal of experimental medicine* 2001;194(6):781-795.

112.   **Hoffmann PR, deCathelineau AM, Ogden CA, Leverrier Y, Bratton DL et al.** Phosphatidylserine (PS) induces PS receptor-mediated macropinocytosis and promotes clearance of apoptotic cells. *The Journal of cell biology* 2001;155(4):649-659.

113.   **de Vries E, Tscherne DM, Wienholts MJ, Cobos-Jiménez V, Scholte F et al.** Dissection of the influenza A virus endocytic routes reveals macropinocytosis as an alternative entry pathway. *PLoS pathogens* 2011;7(3):e1001329.

114.   **Monks J, Rosner D, Geske FJ, Lehman L, Hanson L et al.** Epithelial cells as phagocytes: apoptotic epithelial cells are engulfed by mammary alveolar epithelial cells and repress inflammatory mediator release. *Cell death and differentiation* 2005;12(2):107-114.

115.   **Taja-Chayeb L, Chavez-Blanco A, Martínez-Tlahuel J, González-Fierro A, Candelaria M et al.** Expression of platelet derived growth factor family members and the potential role of imatinib mesylate for cervical cancer. *Cancer cell international* 2006;6:22.

116.   **Dharmawardhane S, Schürmann A, Sells MA, Chernoff J, Schmid SL et al.** Regulation of macropinocytosis by p21-activated kinase-1. *Molecular biology of the cell* 2000;11(10):3341-3352.

117.   **Liang CC, Sun MJ, Lei HY, Chen SH, Yu CK et al.** Human endothelial cell activation and apoptosis induced by enterovirus 71 infection. *J Med Virol* 2004;74(4):597-603.

118.   **Ekstrom JO, Tolf C, Fahlgren C, Johansson ES, Arbrandt G et al.** Replication of Ljungan virus in cell culture: the genomic 5'-end, infectious cDNA clones and host cell response to viral infections. *Virus Res* 2007;130(1-2):129-139.

119.   **Wei T, Kikuchi A, Moriyasu Y, Suzuki N, Shimizu T et al.** The spread of Rice dwarf virus among cells of its insect vector exploits virus-induced tubular structures. *J Virol* 2006;80(17):8593-8602.

120.   **Wei T, Shimizu T, Omura T**. Endomembranes and myosin mediate assembly into tubules of Pns10 of Rice dwarf virus and intercellular spreading of the virus in cultured insect vector cells. *Virology* 2008;372(2):349-356.

121.   **Wei T, Uehara-Ichiki T, Miyazaki N, Hibino H, Iwasaki K et al.** Association of Rice gall dwarf virus with microtubules is necessary for viral release from cultured insect vector cells. *J Virol* 2009;83(20):10830-10835.

122.   **Fu Y, Xiong S**. Exosomes mediate Coxsackievirus B3 transmission and expand the viral tropism. *PLoS pathogens* 2023;19(1):e1011090.

123.   **Roseblade A, Luk F, Rawling T, Ung A, Grau GE et al.** Cell-derived microparticles: new targets in the therapeutic management of disease. *J Pharm Pharm Sci* 2013;16(2):238-253.

124.   **Mediouni S, Mou H, Otsuka Y, Jablonski JA, Adcock RS et al.** Identification of potent small molecule inhibitors of SARS-CoV-2 entry. *SLAS discovery : advancing life sciences R & D* 2022;27(1):8-19.

125.   **Günther S, Reinke PYA, Fernández-García Y, Lieske J, Lane TJ et al.** X-ray screening identifies active site and allosteric inhibitors of SARS-CoV-2 main protease. *Science (New York, NY)* 2021;372(6542):642-646.

126.   **Inal J, Paizuldaeva A, Terziu E**. Therapeutic use of calpeptin in COVID-19 infection. *Clinical science (London, England : 1979)* 2022;136(20):1439-1447.

127.   **Sisa C, Kholia S, Naylor J, Herrera Sanchez MB, Bruno S et al.** Mesenchymal Stromal Cell Derived Extracellular Vesicles Reduce Hypoxia-Ischaemia Induced Perinatal Brain Injury. *Frontiers in Physiology*, Original Research 2019;10(282).

Fig1

Fig. 1

Fig2

Fig. 2

Fig3

Fig. 3
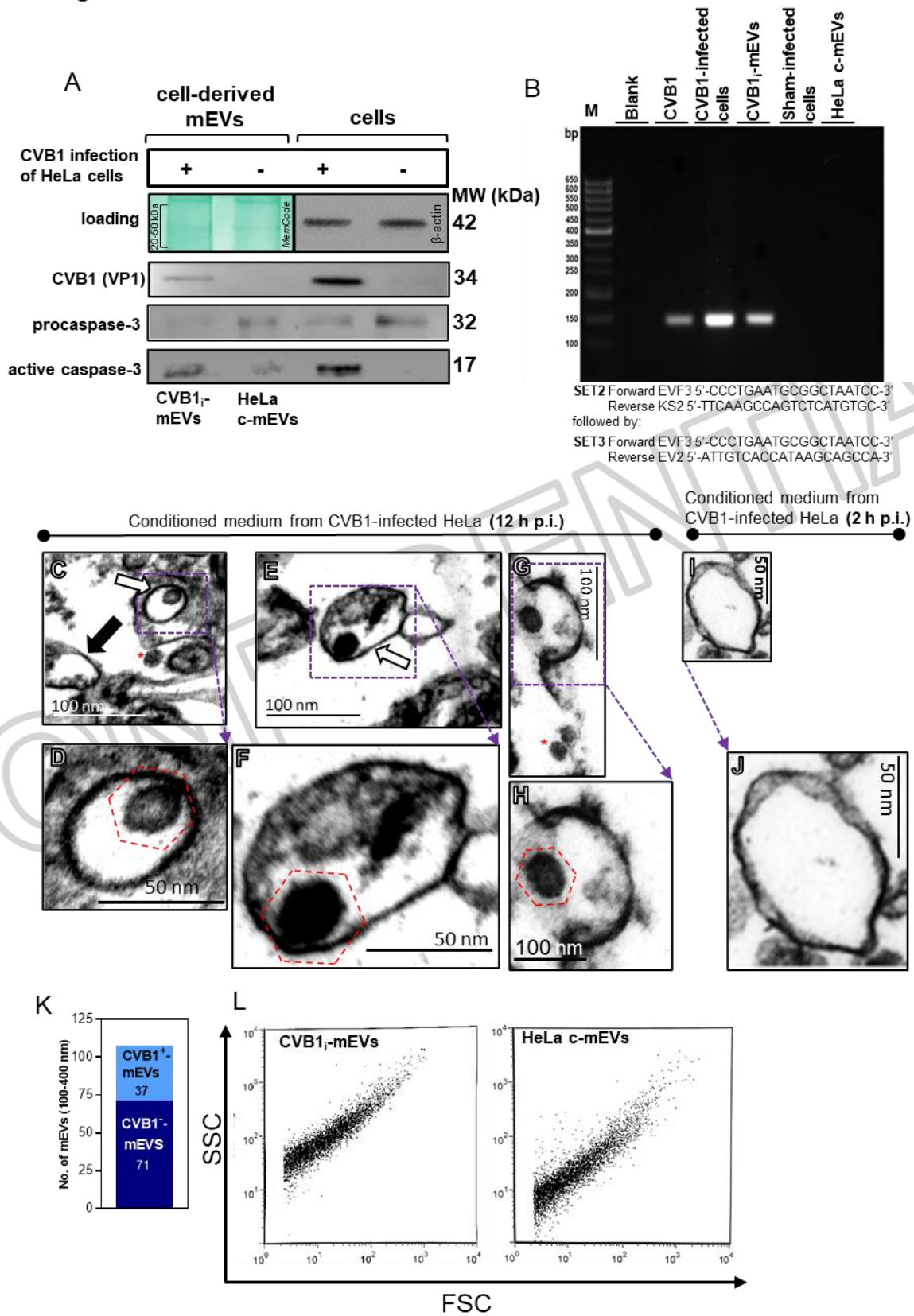

A

cell-derived mEVs   **cells**

CVB1 infection of HeLa cells: + − + −

loading — MemCode / β-actin — 42 MW (kDa)

CVB1 (VP1) — 34

procaspase-3 — 32

active caspase-3 — 17

CVB1ᵢ-mEVs   HeLa c-mEVs

B

M / Blank / CVB1 / CVB1-infected cells / CVB1ᵢ-mEVs / Sham-infected cells / HeLa c-mEVs

bp: 650 600 550 500 450 400 350 300 250 200 150 100

SET2 Forward EVF3 5'-CCCTGAATGCGGCTAATCC-3'
Reverse KS2 5'-TTCAAGCCAGTCTCATGTGC-3'
followed by:

SET3 Forward EVF3 5'-CCCTGAATGCGGCTAATCC-3'
Reverse EV2 5'-ATTGTCACCATAAGCAGCCA-3'

Conditioned medium from CVB1-infected HeLa **(12 h p.i.)**

Conditioned medium from CVB1-infected HeLa **(2 h p.i.)**

C (100 nm) / D (50 nm) / E (100 nm) / F (50 nm) / G (100 nm) / H (100 nm) / I (50 nm) / J (50 nm)

K

No. of mEVs (100–400 nm): CVB1⁺-mEVs 37 / CVB1⁻-mEVs 71

L

CVB1ᵢ-mEVs / HeLa c-mEVs

SSC vs FSC

Fig4

Fig. 4

Fig5

Fig. 5

C. CVB1$_i$-mEVs

D. CVB1

E. CVB1+ CVB1$_i$-mEVs

F. CVB1$_i$-mEVs + CP

G. CVB1 + CP

H. c-mEVs from sham-infected cells

Fig. S1

Fig. S1 Sucrose density gradient purification of CVB1. CVB1 was centrifuged through a 10-25% sucrose gradient (40,000 ×*g* /90 min) and fractionated into 0.5 ml fractions from the top. Fractions 5-8 were pooled and further centrifuged or precipitated with trichloroacetic acid as described in Materials and Methods.
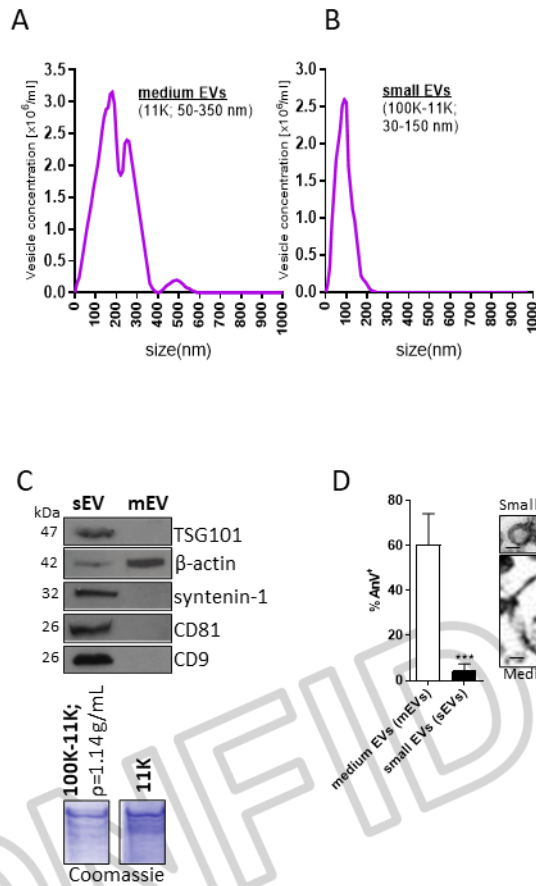
Fig. S2

Fig. S2 mEV (microvesicle) and sEV (exosome) characterisation. (A) NTA analysis shows the size distribution of mEVs (11,000 ×g) isolated from infected HeLa after 12 h (100 – 650 nm) compared to the profile (30 - 240 nm) obtained from an exosome preparation (100,000 ×g minus 11,000 g), (B). Immunoblotting of 11 K and 100 - 11 K pellets (20 µg each lane), shows classic exosome markers in the small EV, sEV ('exosome' pellet) which are absent from the mEV (11,000 ×g) pellet, (C). mEVs showing greater binding with annexin V-FITC than sEVs, was assessed by flow cytometry (mean ±SEM of 3 separate experiments, in triplicate ***P<0.001), and Transmission Electron Microscopy confirms sEV (exosome) and mEV (microvesicle) size difference, Bar = 50 nm, (D).

Fig. S3

siRNA#6 5'-TCC GAC GCT ACT CAG ATG AAA-3'
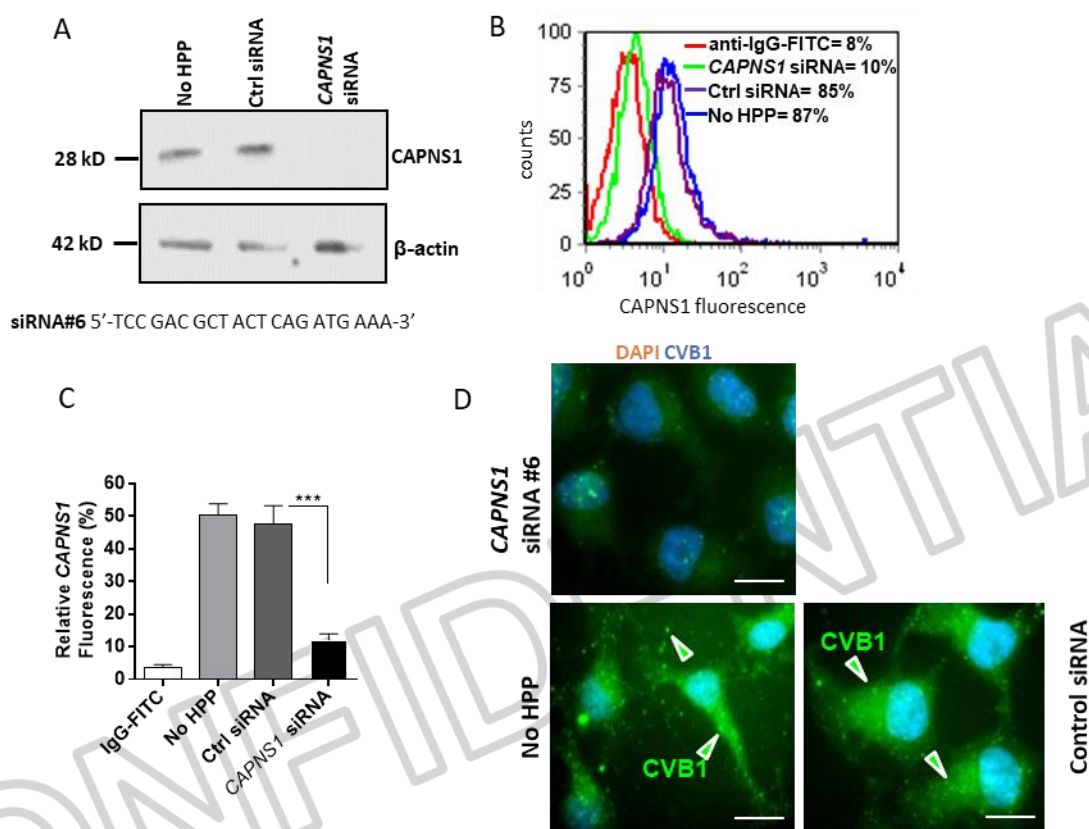
Fig. S3 Silencing of calpain in HeLa cells. Semiconfluent HeLa cells were not transfected (No HiPerfect transfection reagent (HPP)) or transfected with 50 nM of control (ctrl) siRNA or *CAPNS1* siRNA for 12 h. Effective knockdown was assessed by western blotting using 30 μg of protein per lane (A). (B and C), flow cytometry analysis of CAPNS1 knockdown in siRNA treated cells. (D) Immunostaining of CAPNS1 in HeLa cells transfected or not with control siRNA or *CAPNS1* siRNA for 12 h, as analysed by fluorescent microscopy.

Fig. S4
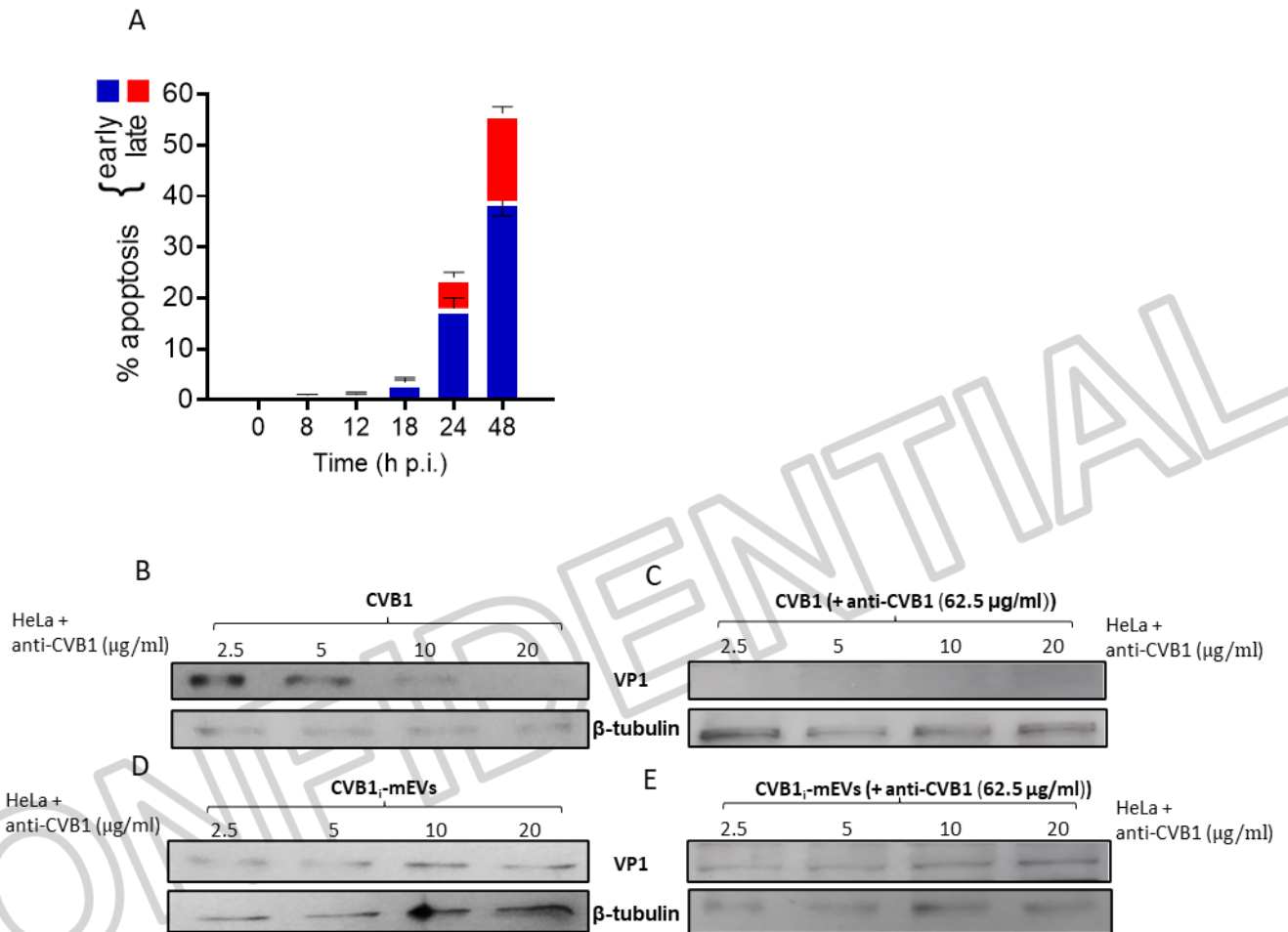
Fig. S4 Time course for CVB1-induced early/late apoptosis in HeLa and during infection with CVB1$_i$-mEV, blocking of any free CVB1-mediated uptake with neutralising anti-CVB1 antibody. (A), Temporal Analysis over 48 h of early (AnV[+]) and late (AnV[+] and 7-AAD[+]) induction of apoptosis by CVB1 (MOI 5.0) in HeLa cells. (B), CVB1 infection of HeLa (detected as VP1 expression) is blocked when HeLa is incubated with increasing neutralising anti-CVB1 antibody. When additionally, CVB1 is incubated with neutralising antibody (C), there is no VP1 expression when CVB1 is incubated even at the lowest concentration of neutralising antibody. In (D) and (E), CVB1$_i$-mEVs infect HeLa in the presence of neutralising antibody against HeLa only (D) or both HeLa and CVB1 (E).
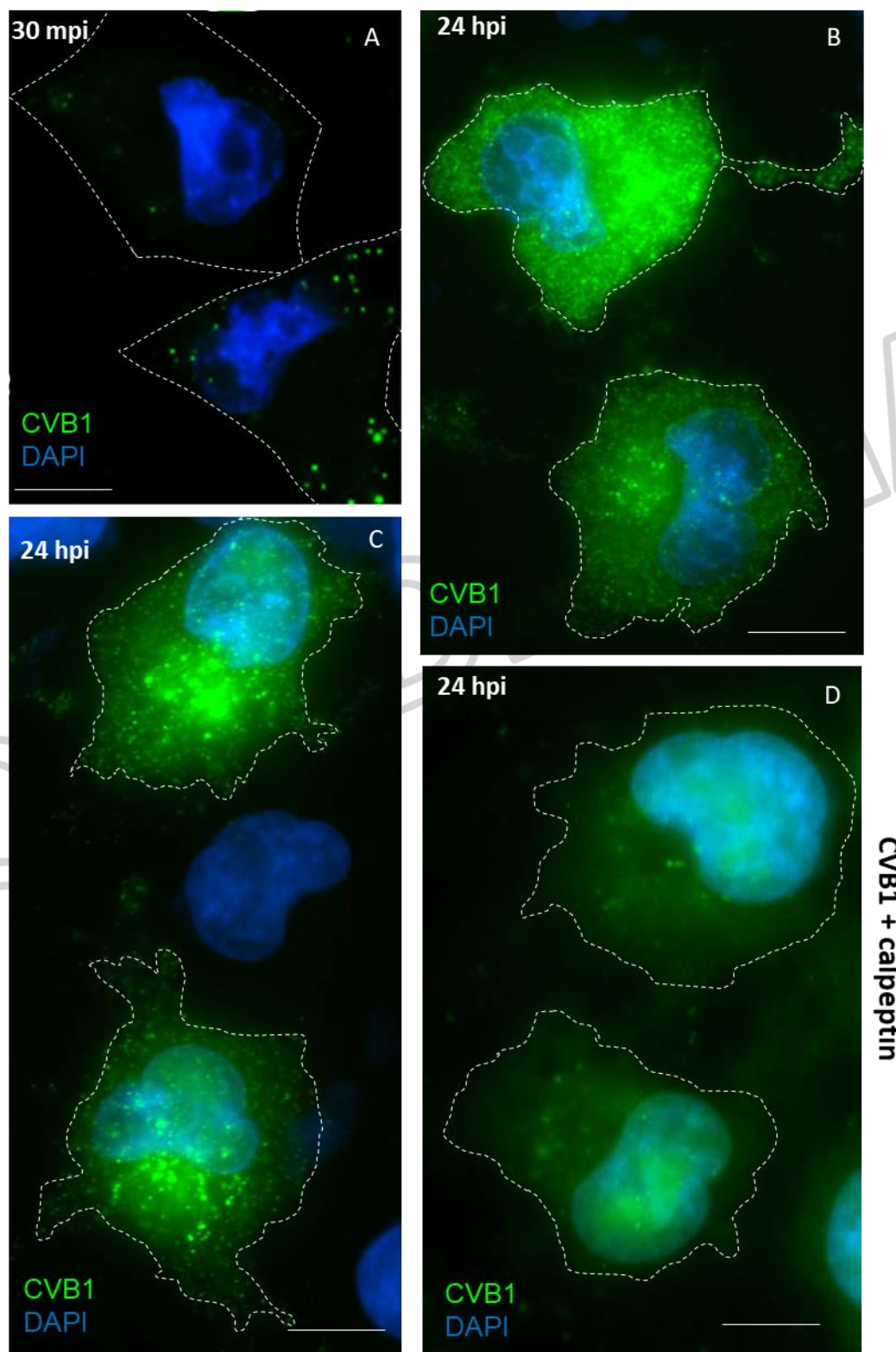
Fig. S5

Fig. S5 mEVs released from CVB1-infected HeLa cells (CVB1$_i$-mEVs) can deliver CVB1 to recipient HeLa cells. (A) Fluorescence microscopy images indicating CVB1 in semiconfluent HeLa cells incubated with CVB1$_i$-mEVs at a ratio of 10 mEVs/cell 30 min p.i. (A) and 24 h p.i. (B). Cells were fixed and permeabilised prior to labelling with mouse anti-CVB1 Alexafluor 488. Nuclei were visualised with DAPI (blue). Images were collected using an Olympus IX81 inverted fluorescence microscope (Olympus Corp, Germany). Scale bar = 10 μm. Representative images are from triplicate experiments.
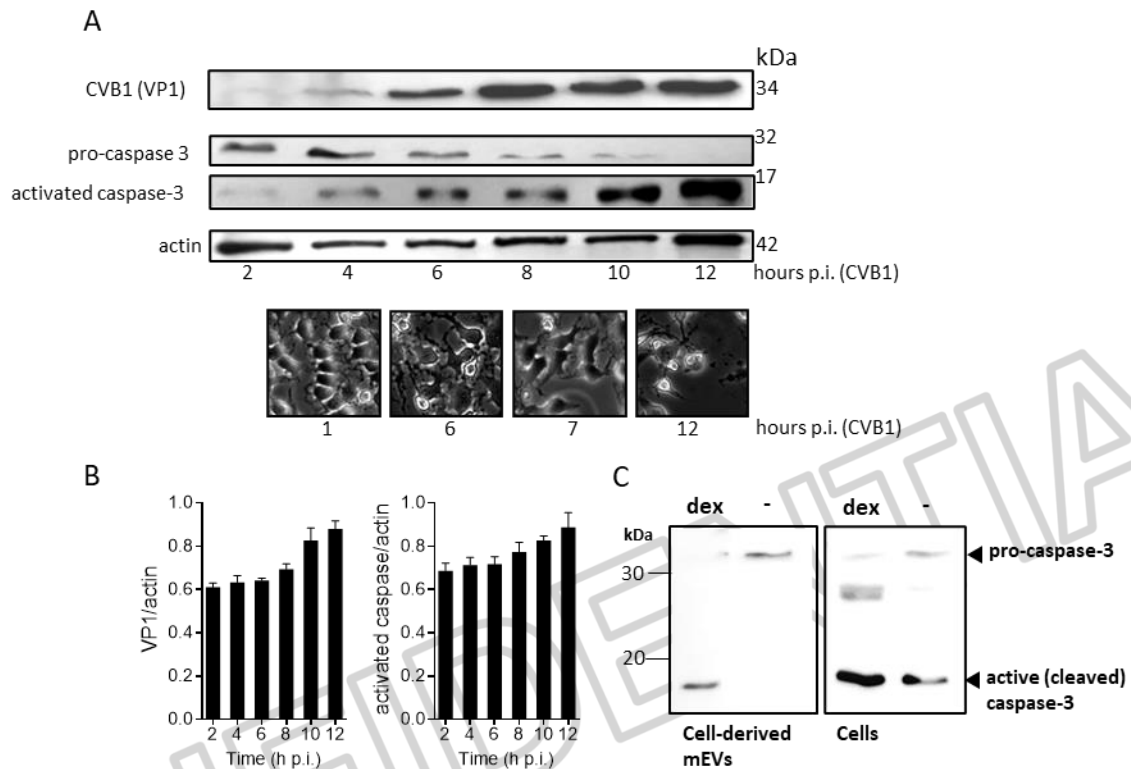
Fig. S6

Fig. S6 Increasing levels of activated caspase-3 and resulting apoptosis after CVB1 infection. Western analysis showed increased levels of activated caspase-3 (A and B) in HeLa cells 8-12 h p.i., as levels of CVB1 (VP1 protein) increase (B). Activated caspase-3 levels were quantified by densitometry using Image J software, relative levels being normalised to actin and expression levels expressed as arbitrary units. In C, apoptosis was induced in HeLa with dexamethasone (DEX) (1 mM; 3 h). Western analysis showed increased expression of activated caspase-3 (and decreased expression of pro-caspase 3) in both DEX-treated cells and in their released mEVs.
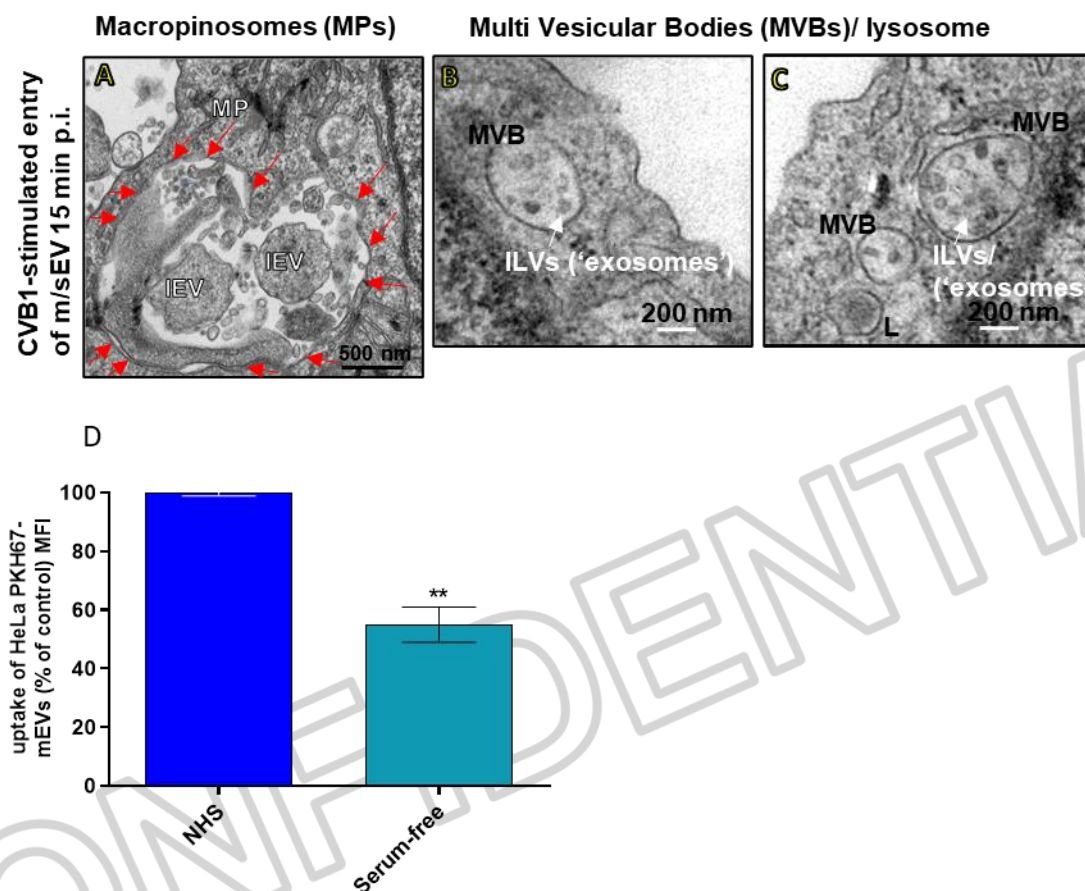
Fig. S7

Fig. S7 CVB1-stimulated macropinocytosis and bystander uptake of mEVs. (A), Macropinosome (MP) visualised in HeLa cells by TEM, delineated by red arrows, showing MP (2 µm in diameter) containing EVs (IEVs and likely sEVs and mEVs). In contrast, (B) and (C) show a smaller multi-vesicular body (MVB) (~800 nm in diameter) containing intraluminal vesicles (ILVs) (~ 80 nm in diameter), later released as sEVs upon MVB fusion with plasma membrane; in (C) an electron dense lysosome can also be seen. (D), Uptake in HeLa cells by CVB1-stimulated macropinocytosis of PKH67-mEVs (CVB1-depleted) measured as mean fluorescence index (MFI) was reduced almost 2-fold in the absence of normal human serum (NHS).
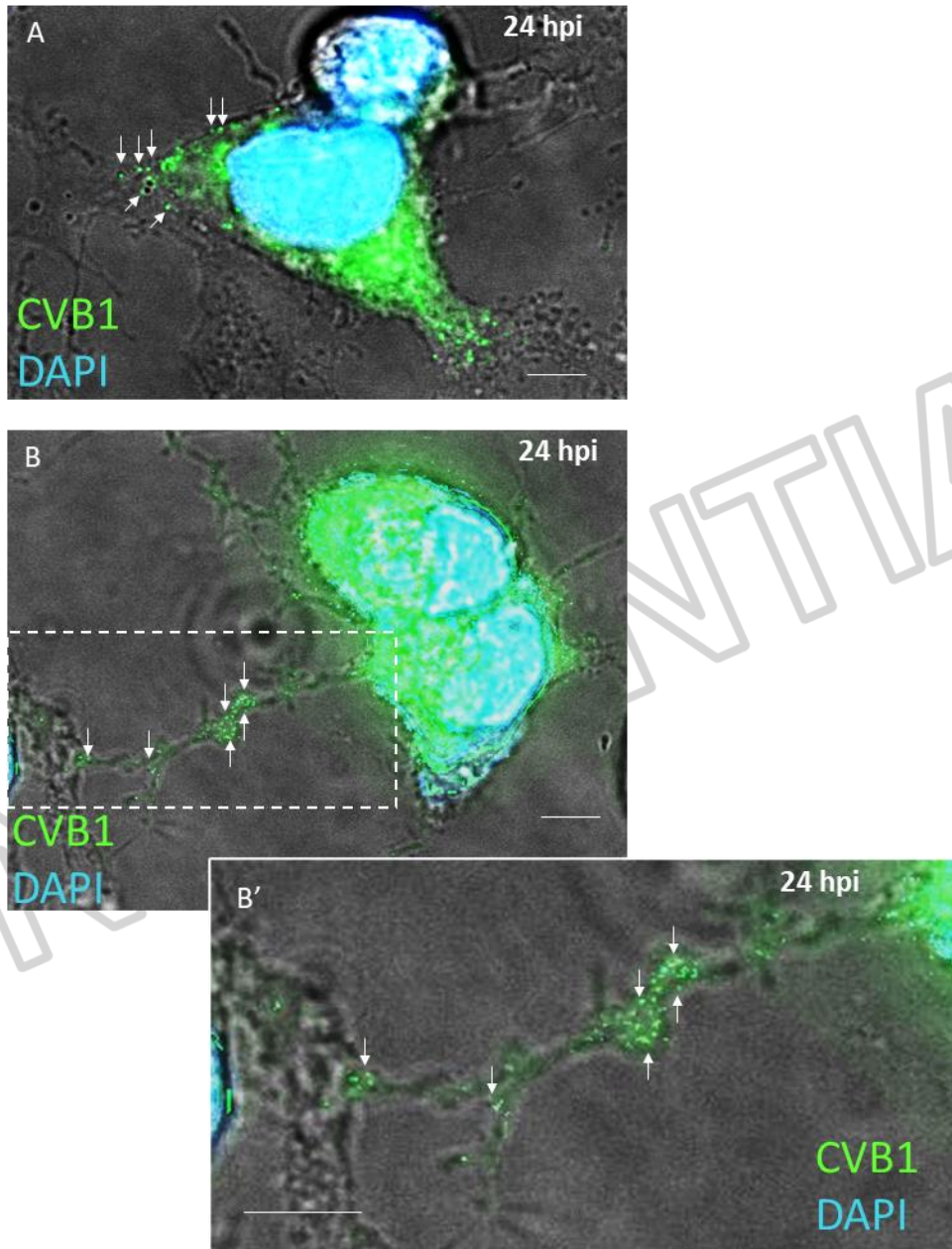
Fig. S8

Fig. S7 Intercellular protrusions between Hela cells with associated CVB1. (A), fluorescent microscopy 24 h p.i. of HeLa cells infected with CVB1$_i$-mEVs. Fixed and permeabilised cells were labelled with anti-CVB1 Alexafluor 488, nuclei counterstained with DAPI and visualised on an Olympus IX81 inverted fluorescence microscope (Olympus Corp, Germany). In (B), an intercellular protrusion connecting two cells is seen which has stained for CVB1. Scale bar = 5 μm. Representative images are from duplicate experiments.